Towards Regenerative Dentistry: Human iOB Differentiation Guided by Single Cell Transcriptomic Atlas of Human Developing Odontoblast.

Sesha Hanson-Drury

A dissertation
submitted in partial fulfillment of the
requirements for the degree of

Doctor of Philosophy

University of Washington
2022

Reading Committee:
Hannele Ruohola-Baker, Chair
Julie Mathieu
Tracy Popowics

Program Authorized To Offer Degree:
Oral Health Sciences

University of Washington

ABSTRACT

Towards Regenerative Dentistry: Human iOB Differentiation Guided by Single Cell Transcriptomic Atlas of Human Developing Odontoblast.

Sesha Hanson-Drury

Chair of Supervisory Committee:

Hannele Ruohola-Baker

Department of Biochemistry

Clinicians, scientists, and the general public share the desire to regenerate missing tooth structure. The majority of mineralized tooth structure is composed of dentin, a material produced and mineralized by ectomesenchyme derived cells, odontoblasts. Though odontoblast development has been characterized in mouse models, mice constantly replenish their missing tooth structure though several stem cell niches not present in human teeth, posing translational challenges between the species. Human odontoblast differentiation and maturation remains largely unknown due to the rarity of tissue samples. To bioengineer missing dentin, increased understanding of human tooth development is required. Thus, our lab performed single cell combinatorial indexing RNA sequencing (sci-RNA-seq) followed by RNA Fluorescence *in situ* Hybridization (RNAScope) of the developing human oral cavity with the hypothesis that:

the dental ectomesenchyme is composed of a heterogeneous cell population that each possess a unique transcriptional signature; changes in expression of these specific transcriptional signatures indicate transitions between cell types; and the molecular mechanisms that drive odontoblast developmental transitions occur at specific spatio-temporal intervals. We found that during early tooth development, the dental ectomesenchyme is divided into two transcriptionally unique components of the tooth germ tissue: the dental pulp composed of dental ectomesenchyme and dental papilla surrounded by the dental follicle. Strikingly, multiple computational assays indicate subodontoblasts (SOB) as a novel odontoblast progenitor source during human tooth development. SOB arise from the dental follicle and transition through a preodontoblast state before giving rise to odontoblasts. Further, we revealed the presence of SOB directly beneath the odontoblasts and intermingled with preodontoblasts at the pulpal periphery. SOB are a source of odontoblast renewal in adult mice following injury, but their presence and role in human odontoblast development has eluded researchers. Thus, our finding identifies this regenerative population in developing humans for the first time and holds incredible promise for SOB as a novel odontoblast progenitor not only during injury repair, but during normal human tooth development allowing us to manipulate and better utilize this naturally regenerating population in human dentistry.

In order to further study odontoblast development, perform disease modeling, and test therapeutic agents, our lab developed an optimized *in vitro* human induced pluripotent stem cell to odontoblast differentiation protocol guided by sci-RNA-seq (iOB). Computational analysis identified fibroblast growth factor (FGF), bone morphogenic protein (BMP), and hedgehog (HH) signaling to play critical roles in human odontoblast

development, with the majority of signaling ligands secreted by neighboring dental epithelium tissues. We found that activating these signaling pathways in induced neural crest cells by treatment with novel AI-designed FGFR superagonist minibinder, BMP ligand BMP4, and HH pathway agonist SAG signaling ligands produces more mature odontoblasts with increased expression of odontoblast markers and enhanced mineralization capacity. This finding implies great potential for AI-designed minibinders as therapeutic agents to induce odontoblast differentiation in clinical cases of pulp exposure or deep caries, as well as generation of mature iOB to be used for tooth organoid generation.

Finally, the congenital disorder Tricho-Dento-Osseous syndrome produces debilitating dental defects associated with mutations in the gene DLX3. While transcription factor DLX3 is known to directly regulate *Dspp* activity and odontoblast development in mice, its role during human odontoblast differentiation is poorly understood. We generated a DLX3 knockout mutant line from HiPSC and tested their capacity to differentiate to mature odontoblasts. Importantly, we identified that DLX3 mutants are able to successfully differentiate towards a neural crest fate, however, odontoblast differentiation is arrested. This indicates DLX3 plays a critical role in early odontoblast development.

The overall significance of this study is threefold: 1) providing unprecedented insight at the single cell level into cell types of the developing tooth dental ectomesenchyme; 2) applying the revealed molecular signaling that controls human odontoblast cell lineage commitment during differentiation to generate a HiPSC-derived odontoblast differentiation method (iOB); 3) utilizing the iOB tool to study the molecular

mechanism of human odontoblast differentiation in states of health and disease in order to design appropriate therapies.

TABLE OF CONTENTS

ACKNOWLEDGMENTS

As The Beatles said, “I get along with a little help from my friends”. This research would not have taken place without the support of many mentors, colleagues and associates. I thank Dr. Justin Teeguarden, for providing me with my first wet-lab research experience and co-authorship for scientific publication, and for writing countless letters of recommendation since. Dr. Richard Darveau, who encouraged me as a pre-dental student to apply for the dual DDS/PhD program due to my passion for science. My dental school classmates, who made our four years in dental school ones of camaraderie and friendship. Dr. Mark Drangsholt, who has been a constant source of guidance and encouragement. KEXP emcees John Richards and Cheryl Waters, who’s music got me through much of my dissertation writing in the gathering space, and Michelle Myers, who let me dance the stress of my dissertation off on Friday Night. Dr. Hannele Ruohola-Baker, who has taught me much about the power of critical thinking and experimental design. The Ruohola-Baker lab members for helpful discussions that propelled this work in new directions. Sydney Kim, Vivian Vo, Druthi Jithendra, Infencia Xavier and Deborah Lee for their excellent technical help. I thank Dr. Mary Reigier for assistance in computational quantification of the RNAScope co-expression channels. Jennifer Dempsey, Ian Phelps, Dr. Diana O'Day from BDRL for processing and collecting the samples from the donors and troubleshooting the nuclei isolation. Dr. Cailyn Suprrell, Aishwarya Gogate and Dr. Lea Starita from BBI for the technical support and overall guidance in the design of the sequencing project. Dr. Jessica Young and Chizuru Kinoshita for their collaboration on the culture of neural crest cells and magnetic cell sorting assay.

DEDICATION

To my friends and family, who have encouraged and supported me on this 17 year journey towards my DDS/PhD. My father, Dr. Rob Drury, who helped me design my first scientific study for the Young Epidemiology Scholars competition. Thank you for your undying love of science and your daughters pursuit of it. My mom, Dr. Sirri Hanson, who has edited every manuscript I have ever written and ingrained in me that I can do hard things. My sister, Tiama Hanson-Drury, for unwavering belief that I will achieve anything I set my mind to, and importantly, to do it with happiness. My husband and partner in life, Toni Munder, for having dinner ready after a long day in the clinic or at the lab, a joke to make a long day lighter, and a bike ride to let off the steam. The wonderful group of dear friends who celebrate my wins and lift me up during my struggles. Lastly, to the patients that I hope to impact with the step forward in regenerative dentistry described in this dissertation.

LIST OF TABLES

LIST OF FIGURES

CHAPTER I - BACKGROUND & SIGNIFICANCE

I.I Odontoblasts produce and mineralize the tooth's dentin, but their progenitors are undefined.

The majority of mineralized tooth structure is composed of dentin, a vital tissue produced and mineralized by odontoblasts. Odontoblast development begins with the migration of cranial neural crest (CNC) cells to branchial arch 1 at gestational week 6 (gw6)[1,2]. Upon arrival, CNC-derived cells condense to form the dental ectomesenchyme, with the preodontoblasts aligned at the periphery of the dental pulp along the epithelial-mesenchymal interface[3]. It has been suggested that during the final cell division of an odontoblast-fate committed cell, one daughter remains in close contact with the epithelial-mesenchymal interface and becomes a preodontoblast; while the other daughter migrates to the subodontoblast Hohl layer with potential to differentiate into new odontoblasts during reparative dentinogenesis[4]. The implication that subodontoblasts give rise to a second wave of odontoblasts during injury is supported by studies that illustrate the capacity to replace lost primary odontoblasts upon tooth injury in rodents[5,6]. Multiple studies have indicated that cells other than the dental ectomesenchyme are capable of giving rise to odontoblasts during injury repair, including mesenchymal stem cells[7] and glial derived stem cells[8]. Further, lineage tracing studies of IGFBP5+ periodontal stem cells indicates this niche gives rise to not only the periodontium but cells within the dental pulp during normal mouse tooth development[9]. The majority of odontoblast progenitor studies utilize the mouse incisor as the study model, as mice constantly wear away their existing dentin, requiring replenishment throughout the animal's lifetime. As human teeth do not possess the same stem cell

niches or regenerative capacity as the mouse incisor, it is a poor comparison for human tooth development and regenerative goals. Therefore, detailed characterization of odontoblast progenitor sources and the capacity of subodontoblasts to give rise to odontoblasts during normal development, not only during injury, remains elusive.

I.II Odontoblast regeneration–is there a public or clinical need?

Replacing lost tooth structure to restore dental form and function has been a clinical goal for over 13,000 years, with one of the earliest examples of dental treatment discovered in a hunter-gatherer of the Late Upper Paleolithic era with a dental filling composed of organic material[10]. The desire to restore the form and function of missing tooth structure remains a prime concern of both clinicians and the general public today. In a recent Reddit thread polling what missing capability of the human body was most desired by community members, tooth regeneration was one of the most upvoted responses. This comes as no surprise to oral health clinicians and scientists alike, as the number of dental patients treated for missing tooth structure is substantial and restorative treatment limitations pose a significant clinical problem.

Tooth structure is commonly lost due to dental caries, trauma, periodontal disease, and congenital defects. The Global Burden of Diseases Study 2017 (GBD 2017) shows that, regardless of gender, oral disorders had the greatest age-standardized prevalence and incidence in the world, persisting in this ranking since 1990[12]. Untreated dental caries is the most prevalent disease globally, with the Center for Disease Control finding that 90% of adults in the United States suffer from dental caries[13]. Further, dental pulp disease was the primary diagnosis for over 400,000 emergency department visits in the U.S. in 2006[14], highlighting the need for significant

resources to restore both the dental pulp and the mineralized dentin tooth structure it produces.

The current method to return form and function to the lost tooth structure (e.g. fillings, crowns) can initiate a continuous cycle of restoration replacement, each replacement leading to increased tooth structure loss due to preparation requirements, recurrent caries, or fracture[15]. This process, known as the “tooth cycle of death”, can ultimately lead to tooth removal and replacement with a dental implant, currently one of the best tooth alternatives. Importantly, after 9 years 45% of dental implants develop peri-implantitis[16], an inflammatory process that can lead to loss of the implant and surrounding bone. At this stage the patient often suffers from insufficient bone levels to support a new dental implant, leaving both the patient and clinician in a treatment quandary. Regenerative dentistry seeks to produce stem cell tools to regenerate missing tooth structure. The need for a tooth organoid is paramount.

I.III Current methods of regenerating dentin tooth structure.

The field of dentistry has a history of pioneering regenerative therapy, with the application of calcium hydroxide to induce reparative dentinogenesis in cases of pulp exposure since the 1800’s[17]. Since then advances have been made in developing therapeutics that lead to more efficient reparative dentin formation. Mineral Trioxide Aggregate (MTA) leads to dentin bridge formation within the pulp. However, as MTA is not biodegradable, dentin formation is limited to within the pulp, preventing replacement of missing tooth structure from extending outward from the dental pulp[18-20]. Biodegradable collagen sponges soaked in WNT agonists delivered to sites of pulpal injury showed increased mineralization compared to MTA in murine models. Importantly,

mineralization extends outside the dental pulp into the access site created by the dental bur[21]. While this finding holds much promise for regenerating lost dentin in vital teeth with a live dental pulp, these methods of dentin regeneration are not applicable to patients with necrotic pulpal tissue. These patients have lost both their primary odontoblasts capable of secreting tertiary dentin and stem cells capable of differentiating to secondary odontoblasts, and thus require a new cell source for pulpal regeneration.

I.IV Barriers to regenerating odontoblasts and dentin tooth structure.

In order to bioengineer missing tooth structure with naturally produced dentin, the following elements are required: a stem cell source, a scaffold, a nutrient source, and small molecule growth factors to direct signaling pathways[22].

The dental ectomesenchyme is rich in stem cell sources, including dental pulp stem cells (DPSC) and stem cells of the apical papilla (SCAP). DPSC have previously been shown to successfully differentiate towards osteogenic and odontogenic fates[23-25] and have been characterized in detail[26]. Unfortunately DPSC expansion and regeneration capacity is limited[27], showing a dramatic decrease in regenerative capacity with increased age[28], and are lost in the case of pulpal necrosis. SCAP are a unique stem cell population present at the tip of the developing tooth root and are hypothesized to give rise to the primary odontoblasts that produce root dentin[29]. SCAP are able to differentiate to odontoblasts *in vitro*[30]. However, SCAP are only present during root development and therefore are not a viable stem cell source in adults[31].

Thus, a large hurdle to developing a clinically translatable method of odontoblast regeneration and tooth organoid formation is the source of stem cells. Human induced

pluripotent stem cells (HiPSC) were discovered by Shinya Yamanaka, who found that he could reprogram mature somatic cells to pluripotency by treating them with 4 transcription factors–*Oct4*, *Sox2*, *Klf4*, and *Myc*–now globally recognized as OSKM factors[32]. HiPSC are capable of giving rise to all cell types of the three germ layers. Thus, they represent a single source of cells to be used to replace those lost to damage or disease. HiPSC are self-renewing, and therefore represent an inexhaustible source of stem cells. HiPSC are generated from adult somatic cells and therefore avoid the ethical concerns of embryonic stem cells. HiPSC eliminate the risk of immune rejection as cells can be derived from an individual patient. HiPSC therefore provide an excellent source of stem cells for regenerative dentistry.

A scaffold is necessary for cells to adhere to and produce their extracellular matrix, as well as provide cell-respective morphology for cell maturation[22]. Dental scientists have explored various biomaterials (e.g. collagen, hyaluronic acid, alginate), with recent studies indicating polylactic acid-*co*-polyglycolic acid (PLGA) polymers to be the primary scaffold selection for dental regeneration due to high porosity and open structure, resulting in increased cell adherence; biodegradable nature; and successful proliferation and differentiation of seeded DPSC[33-36].

Blood vessels serve the critical role of delivering nutrients and oxygen to tissues, as well as removing waste products. Revascularization of the dental pulp can be promoted in immature teeth by inducing bleeding at the root apex, allowing influx of angiogenic cells[37]. However, this method is not successful in necrotic adult dentition, likely due to a lack of stem cell populations able to respond to cell homing. Our lab has dissected the Angiopoietin signaling that guides angiogenesis, finding the application of

computationally designed protein scaffolds induced revascularization following injury[38-40]. This finding holds much promise in application for dental pulp revascularization.

Odontogenesis involves sequential, reciprocal signaling between a diverse cell population originating from the dental epithelium and underlying ectomesenchym[41]. It has been well studied in the mouse incisor that five highly conserved pathways are active throughout tooth development: fibroblast growth factor (FGF), bone morphogenic protein (BMP), sonic hedgehog (HH), wingless-related integration site (WNT), and ectodysplasin (EDAR)[42-43]. For example, the mesenchymal signaling molecule BMP4 regulates the bud-to-cap stage transition. Absence of mesenchymal BMP4 arrests tooth development at the bud stage, while addition of exogenous BMP4 rescues the bud-to-cap transition[44]. FGFR2 knockout mouse models show tooth development arrests at the bud stage[45-46], indicating that FGF signaling is required for normal tooth development. FGF robustly stimulates cell proliferation and cytodifferentiation during tooth morphogenesis, with FGF4 ligand shown to be highly specifically expressed in murine enamel knot[47]. Interestingly, in the primary human dentition, FGF4 has broad expression in both the epithelial and dental ectomesenchyme derived tissues, highlighting the variation between murine and human development[48]. SHH is highly expressed in the inner enamel epithelium and ameloblasts[49], with expression shifting to the odontoblast once dentin is deposited[50], suggesting a role for HH signaling in odontoblast maturation.

The majority of studies on the signaling pathways controlling tooth development have been performed on the mouse incisor, which constantly renews lost tissue due to

stem cell populations, and therefore is not a direct comparative model for human tooth development. The intricate intercellular molecular signaling that regulates human odontoblast development and maturity, and clear markers for the stages of human odontoblast differentiation, remain unknown. Thus, the largest barrier posed to regenerating odontoblasts and dentin tooth structure is the lack of knowledge on the molecular signaling involved in human odontoblast differentiation and the biological markers of odontoblast cells as they mature.

I.V Single cell RNA sequencing of the developing human tooth can provide the missing signaling knowledge needed for odontoblast and dentin regeneration.

Single cell RNA sequencing allows for identification of specific cell types within a heterogenous population and dissection of their lineage projection on a molecular level[51]. Importantly, this ability to discriminate between cell populations has allowed for identification of novel odontoblast markers in the mature human adult dental pulp[52] and dental epithelium of the chronically growing mouse incisor[53], as well as shown conserved gene expression profiles between stem cells of the dental pulp and periodontal ligament, suggesting functional differences are due to environmental niche cues[54]. Due to the rarity of developing human tissue, analysis of the developing oral cavity at single cell resolution is missing, leaving the transcriptomic identities of dental ectomesenchyme derived-cells and the transcriptional effectors that specify progenitor fate and odontoblast differentiation unknown.

I.VI Existing *in vitro* iPSC derived odontoblast differentiation protocols are lacking.

As the need for odontoblast regeneration is critical, previous studies have explored stem cell-derived odontoblast differentiation protocols. In animal models, odontoblast-like cells have been produced from murine iPSC through co-culture with dental epithelium, with the goal of mimicking early tooth development in which the odontoblasts are in close proximity with the ameloblasts[55-56]; and through gene transfection of iPSC to increase BMP4 and PAX9 expression[57]. Both these methods are impractical for therapeutic application as access to developing human oral epithelium is limited and human gene therapy requires further study of off target effects. Interestingly, a recent study found supplementation of murine iPSC derived neural crest like cells with BMP4, FGF8 and WNT3a increases expression of odontoblast marker genes and odontoblast-like morphology[58]. In humans, Xie et al produced iPSC-derived odontoblast-like cells through BMP4 supplementation[59]. Unfortunately, the authors failed to transition through a neural crest state prior to odontoblast differentiation. This gap in odontoblast development misses a crucial stage in odontoblast differentiation, preventing full analysis of odontoblast development and disease modeling. The need for an efficient HiPSC derived odontoblast differentiation protocol remains for tooth regeneration and tooth development studies.

I.VII Beyond dental regeneration, *in vitro* iPSC odontoblast differentiation serves as a tool for disease modeling and developing therapeutics.

A method of producing functional odontoblasts from HiPSC has applications that extend beyond bioengineering lost tooth structure. This tool serves as a model essential to study genetic diseases affecting dentin formation, such as Tricho-Dento-Osseous (TDO) syndrome, as well as develop clinically translational therapies. TDO is a rare but

highly penetrant autosomal dominant disorder associated with mutations in the homeodomain transcription factor gene DLX3[60]. Individuals with TDO suffer from ectodermal dysplastic defects in hair, teeth, and bones[61-62]. TDO produces debilitating dental defects leading to increased dental caries and fracture, resulting in high risk of pulpal necrosis and tooth loss. During early tooth development, *Dlx3* is expressed in cranial neural crest cells of the branchial arches[63]. Loss-of-function studies in mice show that *Dlx3* directly regulates transcription of *Dspp* by binding to the promoter region; DLX3 knock out mutants exhibit downregulation of *Dspp* and dentin defects[64]. Cytodifferentiation of odontoblasts in mouse DLX3 knock-out models is disrupted, leading to impaired dentin production and odontoblast apoptosis[65]. Interestingly, DLX3 inhibits proliferation of human dental pulp cells and has been proposed to play a role maintaining quiescence of this cell population[66]. The role of DLX3 in human odontoblast maturation has yet to be fully explored due to a lack of a developing human odontoblast model. In order to develop TDO therapies, it is critical to deepen our understanding of DLX3's role in human odontoblast development.

CHAPTER II - MATERIALS & METHODS

II.I Single cell RNA sequencing of the developing human oral cavity.

Human fetal tissue collection and dissection. Fetal cranial facial tissues were provided by the Birth Defect Research Laboratory University of Washington after obtaining an informed consent from the patient or legal guardian. This study was approved by the Human Subjects Division of the University of Washington (HSD#51634-EJ) and all methods were performed in accordance with the relevant guidelines and regulations.

The tooth and salivary gland samples were collected from five fetal age groups representing the following developmental stages for tooth differentiation: the bud stage (gw9-11), the cap stage (gw12-13), the early bell stage (gw14-16), and the late bell stage (gw17-22)[42,67]. Tissues were transferred from the BDRL submerged in Hank's Balanced Salt Solution media (Gibco 14025092) on ice. The tissues were further dissected under a dissection microscope to isolate tooth germs, or salivary glands, while still submerged in cold RNase free Phosphate-Buffered Saline (PBS) (Invitrogen AM9624) within six hours from the initial dissection at BDRL. Samples that exceeded that time were excluded from single cell analysis and instead used for histology and immunostaining. Extracted tissues were transferred into Eppendorf tubes and snap frozen using liquid nitrogen. The frozen samples were stored at –80°C until nuclei extraction.

Single cell RNA sequencing. Single cell combinatorial indexing RNA sequencing (sci-RNA-seq) was performed in collaboration with the Brotman Baty Institute and has been described in detail previously[68]. Briefly, cells undergo split-pool barcoding to uniquely label each cell within the entire population of single cells. The first level of

indexing occurs as permeabilized nuclei are distributed across a 96-well plate, then each well receives a specific unique molecular identifier (UMI) incorporated through reverse transcription, barcoding each cell within the well. UMI labeled cells are then pooled and redistributed to multiple 96-well plates for introduction of a second well-specific identifier incorporated through PCR amplification. Amplicons are then pooled for parallel sequencing, producing a transcriptomic library composed of cells identified by their unique combination of barcodes.

sci-RNA-seq data processing. Low quality reads were removed by filtering UMI reads higher than 1500 and lower than 100, followed by removal of all mitochondrial reads. Utilizing the Monocle 3 workflow described previously[69-70] data underwent normalization by size factor, preprocessing, dimension reduction into Uniform Manifold Approximation and Projection (UMAP) space[71], and unsupervised clustering producing grouping of the cells into clusters based on similarity of gene expression, as done previously[68].

Dental ectomesenchyme derived cell population identification. Epithelial and mesenchymal derived cells of the anterior jaw and incisor tooth germ were identified by expression of oral epithelium specific markers KRT5[72] and PITX2[73] and dental ectomesenchyme specific markers PRRX1[74] and RUNX2[75]. The developing jaw ectomesenchyme, dental ectomesenchyme, and odontoblast cells were subset to identify the dental ectomesenchyme derived cell types.

Heatmap and Gene Ontology (GO) terms enrichment. The package ComplexHeatmap[76] was used to generate custom heatmaps that integrate Gene Ontology (GO)-terms for each cluster. GO-terms were generated using the ViSEAGO package[77], which utilizes the top 50 marker genes per cluster as input to determine associated GO-terms. The

GO-terms were sorted by p-value, the top 100 selected, and keywords extracted via simplifyEnrichment package[78]. Keywords were filtered to eliminate redundant and irrelevant terms. Age Score is calculated by normalization of the cell count per time point.

Pseudotime and real-time analysis. Cell lineage trajectories and pseudotime were produced using Monocle 3. Pseudotime is calculated from dynamic changes in differentially expressed genes (DEG) and defines a cell's progress along the developmental trajectory[69].

Cell cycle scoring. Cells were categorized into cell cycle phase according to expression of G2/M and S phase markers as described previously[79].

Regressing out the cell cycle effect. The cell cycle effect was regressed out as described previously[80] by simple linear regression using Seurat[81].

Identification of critical signaling pathways via Top Pathway analysis. Our lab has developed a comprehensive analysis pipeline to evaluate signaling pathway activity based on ligand-receptor interactions and downstream activity. Prior to analysis, a differentiation trajectory with known progenitor, maturely differentiated target cell, and neighboring support cells present at the same developmental stage should be known. Dental epithelium derived cells were included as sources of ligand producing cells. This pipeline utilizes the *talklr* package[82] to identify and rank incoming ligand signals to the progenitor cell of interest (e.g. dental papilla and preodontoblast), filtering for ligand-receptor interactions associated with major signaling pathways of interest (e.g. FGF, BMP, HH). Each interaction is assigned a normalized interaction score, which is calculated by dividing the sum of interaction scores across all pairwise cell-cell

interactions. We then utilized the DEsingle package[83] to produce the DEG between the progenitor and target cells (False Discovery Rate < 0.1 and Fold-Change > 2). We next used scMLnet package to generate a multilayer network modeling the upstream ligand-receptor pairs (from talklr) and downstream transcription factors (TF) and their target genes (from DESingle). Connectivity of each layer of the model was scored to predict which pathway is the most active. Scores were calculated by determining target gene fold-change; mean TF-target genes associated with a given TF; sum of TFs associated with a given receptor; sum of receptors associated with a given ligand; and finally sum of ligands that are associated with a given signaling pathway. Score normalization is performed at each layer. Finally, the pipeline ranks signaling pathways by activity score, indicating the most active pathways including the key drivers of differentiation between progenitor and target maturely differentiated cells.

Code availability. The custom R codes used to generate some of the results in this dissertation are available in https://github.com/Ruohola-Baker-lab/Tooth_sciRNAseq.

II.II Validation of sci-RNA-seq computational findings *in situ* in the human tooth germ.

Crysectioning of developing human tooth germs. tooth germs embedded in optimal cutting temperature compound were cryosectioned to 10 µm sections. Following sectioning, slides were stored at -80℃ and warmed at room temperature prior to staining.

RNAScope assay and confocal imaging. RNAScope assay was performed as described in detail previously using the RNAScope HiPlex12 Reagent Kit v2 (ACD)[84]. Briefly, a 12-probe RNAScope HiPlex assay (Advanced Cell Diagnostics, Inc.) including probes

against 13 transcripts differentially expressed between cell type clusters in ectomesenchyme- and epithelial-derived lineages were selected to distinguish cell populations: VWDE, SALL1, FGF4, IGFBP5, FGF10, PRRX1, FBN2, ENAM, PCDH7, SOX5, KRT5, and either DSPP or LGR6. (Table 1). Cryosectioned tooth germ sections were fixed for 1 hour in 4% PFA at room temperature then rinsed with PBS. Sections were dehydrated by sequential treatment with 50%, 70% and 100% ethanol, followed by permeabilization via Protease IV to allow probe access. Probes were then hybridized by incubation in the HybEZ Oven for 2 hours at 40℃, and rinsed twice in 1X Wash Buffer for 2 minutes. Following hybridization of the probes, the signal was amplified by sequential incubation of RNAscope HiPlex Amp 1-3, each amplification for 30 minutes at 40℃. Autofluorescence was reduced by treatment with Formalin-Fixed Paraffin-Embedded Reagent for 30 minutes at room temperature. HiPlex Fluoro T1–T4 were then hybridized for 15 minutes at 40℃. Nuclei were stained using DAPI and slides were mounted using ProLong Gold Antifade Mountant. All incubations not performed at room temperature were done via the HybEZ Oven.

Table 1. RNAScope Probe Sequences.

Gene	Cluster	Relative expression
SALL1	SOB	1.603378639
FGF4	EK	2.072977626
IGFBP5	SOB	2.0953
FGF10	DP	2.342748687
PRRX1	DEM	2.394496229
FBN2	POB	2.405502878
PCDH7	SI-2	2.478646553
SOX5	DP	2.767965189
KRT5	PAN-DE	2.805817869
VWDE	AM	2.826717442
DSPP	OB	3.019020124
ENAM	SAM	6.316622834

RNAScope imaging and analysis. The first four probes were imaged after completing the manufacturer's specified hybridization steps, counterstaining, and coverslipping. Images of tissue sections were obtained using an Nikon Ti2 with an Aura light engine (Lumencor, Beaverton, OR), and BrightLine Sedat filter set optimized for DAPI, FITC, TRITC, Cy5 & Cy7 (Semrock, Rochester, NY: LED-DA/FI/TR/Cy5/Cy7-5X5M-A-000). Coverslips were removed, the first four fluorophores were cleaved, and the process was repeated for probes 5-8 and then probes 9-12. Images were analyzed using Fiji (ImageJ2 v2.3.0) and QuPath (v0.3.0) quantitative pathology and bioimage analysis freeware[85]. Briefly, The DAPI channel images for imaging rounds two and three were aligned to the DAPI image for imaging round one using the BigDataViewer > BigWarp plugin in Fiji. Matching reference points were identified across the DAPI images and the resultant landmark tables were used in a custom .groovy script to align the FITC, Cy3, Cy5, and Cy7 images from the three rounds of imaging. Images were uniformly background corrected and scaled. Cellular segmentation was performed in QuPath and positive signal foci and clusters were identified as subcellular detections. Parameters were set to allow for detection of foci while avoiding false positive detection events using positive and negative control images. From QuPath, the coordinates and the number of spots estimated (sum of individual puncta and estimated number of transcripts for clustered signal) for each segmented cell were processed using custom R scripts to map cell locations and expression levels. Out of the transcripts assayed by RNAScope, probe set criteria used to identify a given cell population in RNAScope data was selected based on differential expression across the cell types identified in the

sci-RNA-seq data at corresponding time points. Cells matching expression criteria for a cluster's probe set were designated by cluster color and mapped spatially.

Data availability. The data generated in this study can be downloaded in raw and processed forms from the NCBI Gene Expression Omnibus under accession number (GSE184749). The mouse incisor dataset used for comparison can be downloaded from the accession code GSE146123. Upon publication, raw RNAScope data will be made publicly available on dryad.org (Dryad research data repository). Data can currently be downloaded with the temporary link: https://datadryad.org/stash/share/TiKnbN_96SrgYmHHJ7kHa4kH8AYjAFcMXG0BsMlVOeE.

Immunofluorescence protein staining and confocal imaging. Tissue sections and cultured cells were fixed in 4% paraformaldehyde (PFA) then immersed in 1X phosphate-buffered saline (PBS) for 3 X 5-minute washes. Antigen retrieval was performed using 10X Citrate Buffer (Sigma-Aldrich) in a capped coplin jar microwaved for ~45 seconds followed by 15-minutes incubation in the microwave. Slides were then washed in PBS at room temperature for 7 minutes. Slides were blocked for 90 minutes at room temperature in a humidified chamber with a blocking buffer consisting of 0.1% Triton X-100 and 5% Bovine Serum Albumin (BSA) (VWR). The primary dentin sialophosphoprotein (DSPP, Santa Cruz Biotechnology), ameloblastin (AMBN, Santa Cruz Biotechnology), and amelogenin (AMELX, Santa Cruz Biotechnology) antibodies were used at a 1:50 concentration, in conjunction with the primary keratin 5 antibody (KRT5) at 1:100. The primary AP-2α transcription factor (AP-2α, Abcam) was used in conjunction with the primary Nerve growth factor receptor (p75 or CD271,

ThermoFisher) at a 1:500 concentration. The primary antibodies were incubated overnight at 4℃ in a humidified chamber. After 3 X 5-minute washes in PBS in a coplin jar, the slides were transferred to a humidified chamber with secondary antibodies. Secondary antibodies goat anti-rabbit 568 and goat anti-mouse 488 (1:250, Molecular Probes) were applied for 75 minutes at room temperature in the same blocking agent. Slides were then rinsed with PBS 4 X 10-minute washes in a coplin jar. DAPI (1:50, Molecular Probes) was applied for 10 minutes at room temperature in PBS. Slides were then rinsed with PBS for 10 minutes in a coplin jar. Slides were then mounted with Vectashield (Vector Labs) and stored at 4℃ until used for imaging. Confocal Imaging was done on a Leica TCS-SPE Confocal microscope using a 40X objective and Leica Software. Images were processed with Fiji software distribution of ImageJ v1.52i[84-85]. Negative controls were performed substituting PBS.

II.III Human induced pluripotent stem cell (HiPSC) culture and differentiation.

HiPSC culture. HiPSCs line WTC-11 (Coriell, #GM25256)[88-89] are seeded on 6-well plates and cultured in mTeSR1 stem cell medium (StemCell Technologies, #85850) with daily media changes until cells reach ~70% confluency as described previously[90]. mTeSR is a feeder-free maintenance media designed to support a pluripotent state by including key molecules insulin to promote cell survival and proliferation, bFGF for self-renewal and expansion, and TGF to inhibit reprogramming[91]. ROCK inhibitor (ROCKi) (Stemcell Technologies) is added to mTesR for initial 24-hours. To maintain HiPSCs and prevent fusing or premature differentiation of colonies, regular observation under low-power microscopy will be performed with colony passaging as necessary.

HiPSC derived neural crest differentiation (iNC). This project applies the protocol previously described to produce iPSC derived neural crest (iNC) through dual SMAD inhibition and early WNT activation[92] (Fig.5A). HiPSC are seeded at 32,000 cells per well on 6-well matrigel coated plates and maintained in mTeSR until 70% confluent. Differentiation is induced (Day 0) with addition of Basal Neural Maintenance Media (BNMM), which consists of 250 mL DMEM/F12 + glutamine (Gibco 11320-033) and 250 mLneurobasal media (Gibco 21103-049) supplemented with 2.5 mL N2 (Gibco 17502-048), 5 mL B27 (Gibco 17504-044), 2.5 mL GlutaMax (Gibco 35050-061), 2.5 mL ITS-A (Gibco 51300-044), 400 µL 2-Mercaptoethanol (Thermo Fisher 21985023), and 2.5 mL NEAA (Thermo Fisher 11140050). On Day 0, BNMM is supplemented with 10 µM SB 431542 (Biogems BG6675SKU301) and 1 µM LDN 193189 (Biogems BG5537SKU106) for dual SMAD inhibition; inhibition is maintained until Day 4 and Day 3 respectively. On Day 2, WNT is activated via supplementation with 3 µM CHIR 99021 (Tocris Bioscience 4423), which is maintained until Day 11. Media change occurred daily.

Magnetic cell sorting for p75+ iNC. On Day 11, cells were lifted via Accutase (Sigma-Aldrich A6964) and resuspended in an IMAG buffer consisting of 0.5% bovine serum albumin and 2mM EDTA. iNC were isolated with addition of PE conjugated p75 (also known as Nerve Growth Factor Receptor, NGFR, and CD271) antibody (Thermo Fisher 12-9400-42) and Anti-R-PE magnetic beads (BioSciences 557899). p75+ cells were eluted, resuspended in media, and plated on 24-well matrigel coated plates at a density of 250,000 cells per well.

iNC derived odontoblast differentiation (iOB). This project applies the DPSC-derived iPSC to odontoblast protocol previously described by our lab[26], modified to reflect the full signaling pathway activities as detected by our sci-RNA-seq analysis (Fig.4A; Fig.5E). p75+ iNC were cultured in Odontogenic Medium (Day 12), which consists of DMEM + Glutamax (Gibco 10566016), 100nM dexamethasone (Sigma-Aldrich D4902), 10% fetal bovine serum, 5mM b-glycerophosphate (Sigma-Aldrich G9422), and 50 µg/mL L-ascorbic acid (Sigma-Aldrich A4544). Media was supplemented with 100 ng/mL BMP4 (Stemcell Technologies 78211) and either basic FGF (bFGF or FGF2), FGF8b, or FGFR minibinders C1 or C6 for 8 days (D0-D7), followed by 50 ng/mL BMP4 and 400 nM SAG (Stemcell Technologies 73412) for 7 days (D8-D14).

All cultures were performed on Matrigel coated plates at a 1:30 dilution and incubated at 37°C and 5% CO_2 concentration. Each differentiation was performed in triplicate with undifferentiated HiPSC as negative control.

Real-time quantitative reverse transcription-polymerase chain reaction (QPCR). To analyze gene expression, cells were dissociated and lysed with Trizol (Life Technology) with cell pellets stored at -80 °C. RNA purification is performed via TURBO DNA-free™ Kit (Invitrogen) or Aurum™ Total RNA Mini Kit (Bio-Rad), purity and concentration quantification via Nanodrop ND-1000 (Thermo Fisher Scientific). cDNA synthesis via iScript™ cDNA Synthesis Kit (Bio-Rad) or Applied Biosystems™ High-Capacity cDNA Reverse Transcription Kit (Thermo Fisher Scientific), and QPCR performed using oligonucleotide primers for neural crest and odontoblast markers (Table 2), SYBR Green reporter (Applied Biosystems) and 7300 Real-Time PCR System (Applied Biosystems). All QPCR reactions were performed in triplicate, normalized to β-actin and

HiPSC, and assessed using the comparative change in threshold cycle (DDC_t) method.

Table 2. QPCR Primer Sequences.

Cell Type	Primer	Forward Sequence ($5^1 \rightarrow 3^1$)	Reverse Sequence ($5^1 \rightarrow 3^1$)
Endogenous control	β-ACTIN	TCCCTGGAGAAGAGCTACG	GTAGTTTCGTGGATGCCACA
Neural crest	SOX10	CTGGACACTAAACCCCTGCC	CATGTGGACTGGGCTGCAGAC
	PAX3	TGTTTCCCTTTCCTGTGTGG	TTATATCGCCTTGGGCATTG
Odontoblast	MSX1	CTCGTCAAAGCCGAGAGC	CGGTTCGTCTTGTGTTTGC
	DSPP	GAGCAACACGGATGGATGATTTC	CACTCTTGTCACGCACAGCCTTA
	S100A13	TTGAACTCGTTGACGCTGAGG	GCAGAACCACTGACAGAGCTA

Statistical analysis. DDC_t values of gene expression of differentiated samples are compared to undifferentiated HiPSC cells (N=3) and analyzed for significance using Student's *t* test via GraphPad QuickCalcs (www.graphpad.com).

Mineralization capacity assay. Alizarin red staining (ARS) (Sigma-Aldrich TMS-008) is performed to assess extracellular calcium deposition. Culture medium was aspirated from each well and cells washed with PBS 3X. Cells were fixed in 4% PFA for 15 minutes at room temperature. PFA was removed and cells washed 3X with diH_20. diH_20 is aspirated off and 1 mL 2% ARS was added per well. Plates were incubated, covered in aluminum foil, at room temperature for 45 minutes with gentle shaking. ARS was removed and cells washed 5 X with diH_20. Staining was then visualized under phase contrast microscopy (Olympus IX70 microscope, Japan). Stain was released with 10% acetic acid and neutralized with 0.1 M ammonium hydroxide. Stain quantification for OD405 was then performed via Wallac EnVision system.

II.IV DLX3 mutant line generation using CRISPR-Cas9.

DLX3 knockout mutant line generation. Guide RNA (sgRNA) was designed to target the early coding region of the DLX3 gene. Ribonucleoprotein (RNP) complex was prepared

by combining DLX3 sgRNA and the Cas9 enzyme. RNP was then delivered to HiPSC via Amaxa nucleofector[93].

Validation of Cas9 nuclease activity. Genomic DNA was harvested from mutant cells using DNAzol (Thermo Fisher 10503027) and amplification of the DLX3 target DNA was performed via Phusion Flash High-Fidelity PCR Master Mix (Thermo Fisher F548L) supplemented with 3% DMSO. Amplification of the DNA product was confirmed by gel electrophoresis. DNA product was isolated via Monarch Gel Extraction kit (NEB T1020S) and purified DLX3 DNA product was then assessed via Sanger sequencing (Genewiz).

Clonal isolation. Individual clones were isolated and screened for indel mutations resulting in a frame shift leading to a premature stop codon, leading to genetic knock-out of DLX3.

Total protein isolation. Media was aspirated and cells were gently rinsed with 1x PBS. Cells were lysed with 130 µl of lysis buffer containing 20 mM Tris–HCl (Sigma-Aldrich, 1185-53-1) (pH 7.5), 150 mM NaCl, 15% glycerol (Sigma-Aldrich, G5516), 1% triton (Sigma-Aldrich, 9002-93-1), 3% SDS (Sigma-Aldrich, 151-21-3), 25 mM β-glycerophosphate (Sigma-Aldrich, 50020-100G), 50 mM NaF (Sigma-Aldrich, 7681-49-4), 10 mM sodium pyrophosphate (Sigma-Aldrich, 13472-36-1), 0.5% orthovanadate (Sigma-Aldrich, 13721-39-6), 1% PMSF (Roche Life Sciences, 329-98-6), 25 U benzonase nuclease (EMD, 70664-10KUN), protease inhibitor cocktail (PierceTM Protease Inhibitor Mini Tablets, Thermo Scientific, A32963), and phosphatase inhibitor cocktail 2 (Sigma-Aldrich, P5726), respectively, in a tube. Cell lysate was collected in a fresh Eppendorf tube. 43.33 µl of 4× Laemmle Sample buffer

(Bio-Rad, 1610747) containing 10% beta-mercaptoethanol (Sigma-Aldrich, M7522-100) was added to the cell lysate and then heated at 95°C for 10 min. The boiled samples were either used for Western blot analysis or stored at −80°C.

Western blot analysis. The protein samples were thawed and boiled at 95°C for 10 min. 30 µl of protein sample per well was loaded and separated on a 4–10% SDS–PAGE gel for 30 min at 250 Volt. The proteins were then transferred on a nitrocellulose membrane for 12 min using the semi-dry turbo transfer Western blot apparatus (Bio-Rad, USA). Post-transfer, the membrane was blocked in 5% bovine serum albumin for 1 h. After 1 h, the membrane was probed with the respective antibodies: DLX3 (Abcam, AB64953) at 1:500 dilution and β-Actin (Cell Signaling, 3700S) at 1:10,000 dilution. Membranes with primary antibodies were incubated at 4°C, overnight on a rocker. Next day, the membranes were washed with 1X TBST (3 times, 10 min interval). The respective HRP-conjugated secondary antibody (Bio-Rad, USA) at 1:10,000 dilution was added and incubated at room temperature for 1 h. All the membranes were washed with 1× TBST (3 times, 10 min of interval) after secondary antibody incubation and developed using Chemiluminescence developer and imaged using Thermo Scientific CL-XPosure Film or Bio-Rad ChemiDoc Imager.

CHAPTER III - RESULTS

III.I sci-RNA-seq of developing human teeth identifies a transcriptionally heterogenous population of dental ectomesenchyme derived cells.

In humans, oral tissue development begins around 6gw and starts as a thickening in the oral epithelium[41-42,94], giving rise to all primary teeth and salivary gland tissue. Individual teeth develop independently as an extension of the main dental lamina and progress through a series of morphological stages (bud, cap, & bell) within bony crypts of the jaws[95]. Additionally, each developing tooth is surrounded by thick fibrous tissue called the dental follicle[96]. The dental follicle and the tissue it contains comprise the tooth germ[97] (Fig.1A). The oral epithelium will also give rise to the salivary glands (Fig.1A). Like teeth, salivary glands derive from the invagination of a thickened sheet of epithelium into the underlying ectomesenchyme, known as the initial bud stage[98] (Fig.1A).

To better understand early oral differentiation and to dissect how the mesenchymal cell lineages acquire odontogenic competence, we analyzed the developmental gene expression profiles of human fetal stages by single cell sequencing. tooth germ and salivary gland samples were collected from five fetal age groups (Fig.1A-B). These age groups represented the following developmental stages for tooth differentiation: the cap stage (9-13gw), the early bell stage (14-16gw), and the late bell stage (17-22gw) (Fig.1A-E)[42,67]. We also collected submandibular salivary glands from three matched timepoints (12-13gw, 14-16gw, 17-19gw) that cover the pseudo-glandular and canalicular stages for salivary gland development[99] (Fig.1A).

Single-cell sequencing data of the tissue samples were analyzed using Monocle3[68-69] and visualized in uniform manifold approximation and projection (UMAP) space (Fig.1D). The distribution of the cells from each tissue origin was identified by using density plots by tissue type (Fig.1C). Utilizing a graph-based clustering algorithm, we annotated 20 major clusters based on key marker genes (Fig.1E) from PanglaoDB. The major cell types in salivary gland samples include salivary mesenchyme, salivary epithelium, cycling salivary epithelium, myoepithelium, and ductal cells (Fig.1C-D). In the jaw samples (9-11gw, Fig.1C-D) we identified mesenchymal progenitors, osteoblasts, neuronal, Schwann cells, muscle, respiratory epithelium, otic epithelium and oral epithelium (Fig.1C-D). The major cell types in tooth samples include dental ectomesenchyme and epithelium, and odontoblasts and ameloblasts respectively. The cell types observed in all samples include endothelial[101-103] and immune[104-105] cells. Our lab has characterized the developing human salivary gland in detail[106].

To confirm the timing of the tooth morphological stages, we performed immunohistochemistry on tissue sections, and as expected, all the dental epithelium derived tissues were visualized by KRT5 (green) (Fig.1E). There are two critical lineages in tooth development: odontoblasts and ameloblasts. These are the two cell types that secrete the mineralized protective layers that cover the soft dental pulp, which contains the nerves and the nutrient transporting blood vessels. Odontoblasts are ectomesenchyme-derived cells secreting the inner coverage for the pulp, called dentin, while ameloblasts are ectoderm-derived and secrete the outermost layer, enamel. To establish expression of known odontoblast and ameloblast markers in our tissue, immunohistochemistry was performed on human fetal tooth germ at 20gw using dentin

sialophosphoprotein (DSPP) and ameloblastin (AMBN) respectively (Fig.1F-K, Fig.3K-Y). As expected, ameloblasts express AMBN in secretary vesicles (Fig.1I-J), and likewise, odontoblasts secrete DSPP (Fig.1I, K). We further validated expression of ameloblast marker AMELX, observing a mirrored expression pattern between the developing ameloblast and odontoblast (Fig.3A-J).

III.II sci-RNA-seq of developing human tooth identifies a transcriptionally heterogenous population of dental ectomesenchyme derived cells.

To dissect the cells derived from the developing jaw mesenchyme, dental ectomesenchyme, and odontoblast cells were identified by PRRX1, RUNX2 and DSPP expression, respectively, then subset and embedded in UMAP space (Fig.2A and 1B). This analysis identified a heterogenous cell population of six transcriptionally unique clusters including the dental papilla (DP), preodontoblast (POB), odontoblast (OB), subodontoblast (SOB), dental ectomesenchyme (DEM), and dental follicle (DF) (Fig.2C) that were identified by putative marker genes (Fig.1D).

The DEM is identified by increased expression of neural crest derivative marker Paired Related Homeobox 1 (PRRX1)[107] and dental ectomesenchyme marker Runt-Related Transcription Factor 2 (RUNX2)[75]. The DF shows high expression of Insulin Like Growth Factor Binding Protein 5 (IGFBP5)[108], as well as markers recently identified in the adult human dental follicle and periodontal ligament including Periodontal Ligament-Specific Periostin (POSTN), Netrin 1 (NTN1), Podocan Like 1 (PODNL1)[53,109], microfibrillar associated protein 5 (MFAP5), Wnt Family Member 2 (WNT2), and Paired Box 3 (PAX3)[110]. The DP has moderately high expression of PRRX1, an anticipated result as both the DEM and DP are putatively neural crest

derived tissues, but is differentiated from the surrounding DEM by elevated expression of Spalt Like Transcription Factor 1 (SALL1)[53]. DP is further uniquely identified by co-expression of SRY-Box Transcription Factor 5 (SOX5)[111] and Fibroblast Growth Factor 10 (FGF10)[112]. POB cells show maintained elevated expression of SALL1, indicative of their heritage from the DP and previously observed in the mouse incisor[53], with significantly increased expression of Fibrillin 2 (FBN2)[113]. Similar to POB, SOB show moderate levels of SALL1 expression, suggesting a shared functional fate of POB and SOB to give rise to the OB. SOB are specified by high expression of IGFBP5[108] and markers previously observed in the SOB in mouse and rat molar respectively, including transcription factor Hairy And Enhancer Of Split-Related Protein 1 (HEY1)[114], Thy-1 Cell Surface Antigen (THY1)[115], and Alkaline Phosphatase, Biomineralization Associated (ALPL)[116]. Finally, OB are identified by robustly known markers Dentin Sialophosphoprotein (DSPP)[117], Dentin Matrix Acidic Phosphoprotein 1 (DMP1)[116], and Collagen Type I Alpha 1 Chain (COL1A1)[119-120], as well as recently identified S100 Calcium Binding Protein A13 (S100A13)[53](S.Fig.A,G).

To evaluate the function of each cluster, we performed gene ontology analysis using ViSEAGO, which uses data mining to establish semantic links between highly expressed genes in a given cluster. This analysis shows that DP and DEM are characterized by signaling, morphogenesis and adhesion, supporting their role as the precursor populations, while POB are characterized by their projection and proliferation, indicative of their precursor role and alignment to the edge of the dental pulp. SOB indicates activation, growth, and signaling, characteristics of a cell type sensing and

influencing its environment, while OB shows GO-terms toward odontogenesis, tooth, and biomineral (Fig.2B).

To assess progenitor sources and cell's progression towards differentiation, pseudotime trajectory analysis was performed. This analysis indicates two progenitor sources are present within the developing dental ectomesenchyme: the DP that give rise to POB and, subsequently, OB; and the DF that gives rise to SOB, which transition through a POB phase before giving rise to OB (Fig.2C). Pseudotime analysis is supported by real-time density plots that show reduced progenitor type cell population density as the tooth germ develops, indicating fate commitment to OB lineage begins after 13gw in human fetal development and is largely complete by 20gw (Fig.2D). Broad expression of dental ectomesenchyme marker PRRX1 is observed in both the DEM and DP (S.Fig.1C), supporting previous findings[3] that a shared cranial neural crest progenitor gives rise to both DP and DF. Thus, we propose a simplified trajectory of both the odontoblast and dental follicle lineages (red and grey arrows respectively, Fig.2E), with a shared PRRX1+ progenitor giving rise to both DEM and DP.

III.III Developmental trajectory suggests SOB as a novel odontoblast progenitor in human tooth development.

Pseudotime trajectory indicates that two progenitor sources are present within the developing dental ectomesenchyme: the DP that gives rise to POB followed by OB; and the DEM that gives rise to the DF followed by SOB. SOB appear to transition through a POB state before giving rise to OB (Fig.2C). While previous studies have shown that SOB, a spatial subgroup of regenerative mesenchymal cells, can give rise to odontoblast-like cells upon death of the primary odontoblasts[5-6], their developmental

and transcriptional identity remains uncharacterized. These results suggest that SOB lineage can differentiate to OB, not only to replace lost OB following injury as previously observed in animal models, but also during normal tooth development. Pseudotime trajectories are supported by real-time density plots (Fig.2D), showing that OB progenitor DP population density decreases as the tooth germ develops, indicating fate commitment to OB lineage occurs prior to gw19 in human fetal development (Fig.2J,K).

Cell cycle scoring provides important information on progenitor sources and developmental scoring. Our analysis of the dental ectomesenchyme derived tissue supports DP and DEM as progenitor populations, as roughly 50% of cells are in G2M/S phase (S.Fig.1D). It also suggests SOB as a progenitor source of OB during normal tooth development, as this cell type has the highest proportion of cells in G2M/S phase. As anticipated, OB shows low levels of G2M/S phase, indicating its role as a mature cell type that has terminally differentiated.

III.IV Cell types identified by sci-RNA-seq are present at specific spatio-temporal stages of tooth development *in vivo*.

To validate the observed sci-RNA-seq DEG and novel biomarkers, RNAScope *in situ* multiplex hybridization[84] was performed on human incisor and molar tooth germs in early (gw13) and late (gw19) stages of development (Fig.2F and H). This technique has proved incredibly useful in identifying cells that co-express multiple transcriptional markers.

As predicted by computational analysis (Fig.2A,B), dental ectomesenchyme derived cell types display spatiotemporally specific expression patterns. At early tooth development (gw13), the dental pulp consists of SOX5/FGF10/SALL1+ dental papilla

(DP) with PRRX1+ dental ectomesenchyme (DEM) localized to the apical portion (Fig.2F,G,J; S.Fig.1E; S.Fig.2A-G; S.Fig.3A,B). The entire tooth germ is surrounded by dental follicle (DF) cells, a pattern which persists to late tooth development (gw19). Interestingly, during early tooth development a small number of DF cells appear within the dental pulp (Fig.2F,G,J). By late tooth development (gw19) the dental pulp shows an organized hierarchy of cells at the incisal tip, with DSPP+ odontoblasts (OB) present at the incisal edge adjacent to FBN2+SALL1+ preodontoblasts (POB) aligned to the periphery of the dental pulp (Fig.2H,I,K; S.Fig.1F; S.Fig.2H-N; S.Fig.3C,D). IGFBP5+SALL1+ subodontoblasts (SOB) are localized directly beneath the OB and, interestingly, intermingled with the POB at the pulpal periphery, suggesting SOB may transition through a POB-like state. The remaining dental pulp is a mixed population of DP, SOB, and POB with DEM localized to the apical region (Fig.2K).

This analysis identifies a novel biomarker, IGFBP5, for the developing dental follicle (DF) (S.Fig.1A,B; S.Fig3.A-D). Further, we have identified novel human SOB biomarkers SALL1 and IGFBP5 (S.Fig.1A,B; S.Fig2.K,M; S.Fig.3C,D), whose co-expression is spatiotemporally limited to define this cell type at gw19. This analysis reveals for the first time the presence of subodontoblast cells in the developing human tooth. Further, the maintained expression of IGFBP5 from early to late tooth germ development supports the hypothesis that SOB are DF derived cells, and that SOB fate commitment occurs prior to gw13.

Additionally, to assess expression of odontoblast markers at the protein level, immunohistochemical analysis was performed on human incisor tooth germs in early (gw15) and late (gw20) bell stage of development. As predicted by sci-RNA-seq, we

observed specific, spatio-temporal expression patterns that differ markedly from early to late tooth development. Expression of OB marker DSPP and ameloblast (AM) markers AMBN and AMELX begins at gw20. We observed mirrored expression patterns of DSPP, AMBN, & AMELX between the OB & AM, supporting previous findings[72] (Fig.1F-K; Fig.3A-Y).

To summarize, at gw13 the dental pulp consists of majority DP with DEM localized to the apical area, with the entire tooth germ surrounded by the DF. Interestingly, a small number of DF are present within the dental pulp, suggesting these cells have already committed to the SOB lineage at this early developmental stage. By gw19 the incisor pulp contains POB, SOB and OB with a smaller contribution of DEM at the apical foramen (Fig.2J,K). This suggests OBs are mainly derived from POB, while SOB serves as a reserve, with the capacity to differentiate to OB through a POB transitional state (Fig.2C,E). Further experiments will dissect how SOBs may play an inductive role in OB differentiation during tooth development.

III.V Early FGF and BMP activation, followed by HH signaling, are critical to human odontoblast development.

Analysis of the most active signaling pathways during human odontoblast differentiation predict that FGF, BMP, and HH signaling pathways are critical to directing this developmental trajectory. We find FGF and BMP (22%) are most active during DP to POB transition, with BMP activity dropping by roughly half (12%) during POB to OB transition and the majority of signaling derived from HH (22%) (Fig.4A). During the transition from DP to POB, the dental epithelium derived cells are the major source of FGF and BMP signaling ligands including FGF1 and FGF23, which bind to FGFR1

possessing DP cells; and BMP10 that binds to BMPR2 and ACVR2A possessing DP cells, respectively. We observe the dental ectomesenchyme as a smaller source of BMP ligands, including INHBC and GDF5, with a lesser contribution of autocrine signaling to the dental papilla (Fig.4B,D).

During the transition from POB to OB, the main source of BMP signaling ligand is predicted to be from the dental epithelium derived pre-ameloblast (PA) that secretes BMP10 and GDF9, which binds to BMPR2 and ACVR2A on the surface of POB. Interestingly, the subodontoblast (SOB) is the major source of BMP4 ligand, which binds to BMPR2 on the POB (Fig.4C). HH signaling, the most active pathway in the transition, shows significantly increased DHH ligand expression in the PA, which is received by PTCH1 and HHIP possessing POB. FGF ligands are received from both dental epithelium and dental ectomesenchyme derived cells. NOTCH signaling, the third contributing pathway in the POB to OB transition, is largely activated by DLL4 secretion by the PA, received by NOTCH1, 2, and 4 possessing POB; and DLL1 secretion by the OB received by NOTCH1 on POB.

III.VI Early FGF and BMP activation, followed by HH activation, leads to more mature odontoblast development *in vitro*.

To fully capture the developmental trajectory of the human odontoblast, human induced pluripotent stem cells (HiPSC) were first differentiated to a neural crest fate as described previously (Fig.5A). Successful differentiation was confirmed by magnetic cell sorting for neural crest marker p75. 98% of differentiated cells positively expressed p75 (Fig.5B). Differentiation was further validated by immunohistochemical analysis, which showed induced neural crest cells (iNC) express p75 and neural crest marker

transcription factor AP-2α (Fig.5C). Lastly, expression levels of neural crest markers PAX3 and SOX10[121] were assessed at the transcriptional level via QPCR, which indicates significantly increased expression of both markers in iNC (Fig.5D).

Next, iNC were biased to an odontoblast fate by activating the FGF, BMP and HH signaling pathways identified by computational analysis of sci-RNA-seq data (Fig.4A and Fig.5E) via supplementation with AI-designed FGFR minibinder superagonist, BMP ligand BMP4, and HH pathway agonist SAG, respectively (S.Fig.5A). iNC derived odontoblast cells (iOB) have significantly decreased expression of neural crest markers SOX10 and PAX3 (Fig.5F), and increased expression of odontoblast markers MSX1, DSPP and S100A13 compared to undifferentiated HiPSC (Fig.5G). Further, iOB show increased DSPP expression at the protein level (Fig.5H; S.Fig.5B,C) and enhanced mineralization capacity as assessed by Alizarin Red Staining (Fig.5I; S.Fig.5D,E), indicating iOB have reached a mature state.

III.VII Loss of DLX3 arrests odontoblast maturity at the preodontoblast stage *in vitro*.

In order to assess the precise developmental stage at which DLX3 plays a role in human odontoblast development, we generated a DLX3 knock-out line derived from iPSC and differentiated it towards neural crest followed by odontoblast fate as described above. Presence of deletion mutation within exon 2 of the DLX3 gene was confirmed by Sanger sequencing via Genewiz, illustrating that 54% of cells possess a single base pair deletion (indel mutation) at site 374 with removal of a single glycine nucleotide (Fig.6A). It appears that the DLX3 mutant is dominant in a mixed population, as sequencing of DLX3 KO following iNC differentiation shows a population shift to 84% of

cells possessing the indel mutation (Fig.6B). Loss of DLX3 protein was confirmed by Western blot analysis, which showed no band formation validating loss of DLX3 protein (Fig.6C).

Differentiation of DLX3 mutants to neural crest fate appears unaffected by the loss of DLX3, illustrated by no significant changes in percent of p75+ cells produced via magnetic cell sorting (Fig.6D) or neural crest markers PAX3 or SOX10 expression (Fig.6E). Mutants were then further differentiated toward odontoblast fate as described previously. Interestingly, loss of DLX3 results in significantly decreased DSPP expression (Fig.6F), indicating DLX3 plays a critical role in DSPP expression. Further, mutant iOB show significantly inhibited mineralization capacity via Alizarin Red Staining (Fig.6G-H). In the human dental pulp, DLX3 is highly expressed in the POB (Fig.6I), indicating a critical role for this transcription factor in OB development and supporting the hypothesis that loss of DLX3 prevents the transition from POB to mature OB through decreased expression of DSPP.

CHAPTER IV - DISCUSSION & CONCLUSIONS

Odontoblasts are required for formation of the tooth's dentin, which composes the majority of the tooth's mineralized tissue. Dentin provides the tooth's toughness, or resistance to crack propagation, and tensile strength, or distribution of biomechanical forces to the surrounding periodontium. While odontoblasts persist throughout life, their number and ability to produce dentin significantly decreases with age. We identified human dental pulp and follicle cell types that significantly and precisely promote the differentiation of odontoblasts. Importantly, we have identified the subodontoblast as a novel odontoblast progenitor in human tooth development. Analyzing the signaling interaction in odontoblast differentiation allowed us to predict the signaling molecules that are needed to recapitulate odontoblast development *in vitro*. Utilizing these findings, we developed a novel differentiation protocol to drive the differentiation of iPSCs toward odontoblast (iOB) that expresses mature odontoblast markers and secretes mineralized tissue. Finally, we used this information to dissect the role of dentin defect associated DLX3 in odontoblast development, identifying the precise molecular step at which odontoblast differentiation is arrested with loss of this critical transcription factor.

Single cell analysis of the developing dental pulp and follicle identified a group of six transcriptionally unique cell types of dental ectomesenchymal lineage. This analysis identifies novel biomarkers for the dental ectomesenchyme derived cell types in the developing human tooth germ that give rise to mature odontoblasts, characterizing each cell type with a specific transcriptional signature.

The dental papilla (DP) is identified by co-expression of signaling molecule FGF10 and transcription factors SOX5 and SALL1. FGF10 is a growth factor that plays critical roles in cell proliferation, differentiation and migration[104]. In the dental pulp, FGF10 is expressed in the mouse molar DP early in tooth development with decreased expression in the odontoblast, suggesting a role in odontoblast maturation[112]. SOX5 has previously been observed in the mouse molar dental ectomesenchyme at early tooth developmental stages[111] and is known in other tissues to play regulatory roles in both BMP[123] and HH[124] signaling pathways. Crosstalk between the FGF signaling pathway and SOX transcription factors has been observed to impact osteoblast development[125], however, their interaction in odontoblast development remains unknown. SALL1 has previously been observed in the mouse incisor preodontoblast (POB)[53], indicating synchrony of odontoblast progenitor gene expression patterns between murine and human models. Elevated expression of SALL1 in the DP–expression that is maintained in the human preodontoblast, subodontoblast, and odontoblast cells–supports the hypothesis that odontoblast fate commitment occurs prior to odontoblast orientation at the periphery of the pulp.

The developing human preodontoblast (POB) shows a transcriptional signature of increased FBN2 expression and maintained SALL1 expression. Fibrillins are a major component of microfibrils and elastic fibers, structures critical for cellular mechanical stability and regulating cell development by sequestering TGFβ and BMP signaling molecules[126]. FBN2 has been shown to increase in the periodontal ligament in response to mechanical stress[127]. We hypothesize that increased FBN2 expression in the POB supports the dogma that these precursor cells migrate first towards the pulp periphery,

then the incisal edge, before giving rise to OB. Clarifying the role of FBN2 in controlling signaling interactions of the differentiating POB will require further study.

Our findings identify the subodontoblast (SOB) in the developing human tooth germ for the first time, and suggest this cell type as a novel odontoblast progenitor. The SOB is capable of giving rise to odontoblasts during injury repair; in addition to this reparative role, our studies suggest SOB can give rise to OB not only following loss of the primary OB, as previously reported, but during normal healthy human tooth development. This hypothesis is supported by computational analysis of sci-RNA-seq data of the developing tooth germ, indicating 1) shared expression of biomarker SALL1 in dental papilla (DP) progenitor that is maintained in both preodontoblast (POB) and SOB cells at later developmental stages; 2) pseudotime analysis (Monocle3) indicating that SOB transition through a POB state before giving rise to OB; and 3) cell cycle scoring shows 60% of SOBs are actively cycling through G2M/S phases, supporting their role as a source of OB progenitor. Further, *In situ* visualization of SOB finds these cells spatially localized to the subodontoblastic region directly beneath the OB and intermingled with POBs at the periphery of the dental pulp, strengthening the suggestion SOB cells transition through a POB-like state prior to differentiating to OB during normal tooth development.

IGFBPs bind with high affinity to IGF signaling ligands, inhibiting their interactions with IGF receptors[128]. IGFBP5, a highly conserved protein in vertebrate organisms, has previously been shown to regulate cell migration, proliferation, and survival[129-130]. IGFBP5 has been observed in the dental papilla and odontoblasts of mouse incisor and is proposed to play a role in differentiated odontoblasts cell survival

and maintenance[108]. Our observation of localized IGFBP5 expression in the SOB supports the suggested role of IGFBP5 in maintaining a progenitor population that is actively differentiating towards a more mature OB fate. Further studies using lineage tracing methods are needed to verify this exciting hypothesis, revealing if SOBs encompass an inductive role in OB differentiation during human tooth development.

For the first time in human development, our studies have revealed in extreme detail, the signaling pathways that govern each transition between odontoblast cell identity. Previous studies of hypodontia and tooth agenesis have shown that disruption of WNT, BMP, and FGF signals result in defective tooth development. However, the detail with which our study has revealed the role of these pathways at various points in odontoblast development may more mechanistically explain how defects in these pathways lead to tooth loss or tooth agenesis. This study reveals at a molecular level the specific effectors that control human odontoblast development, indicating that FGF, BMP, and HH are the critical signaling pathways contributing to odontoblast differentiation. This knowledge can be used to develop therapeutic agents to induce dentinogenesis clinically and was applied here to develop an efficient HiPSC-derived odontoblast differentiation protocol (iOB).

The single cell based differentiation protocol of iPSC to odontoblast (iOB) produced mature odontoblast cells that showed significantly increased expression of odontoblast markers and enhanced mineralization capacity. While odontoblasts persist throughout life and are able to respond to injury by secreting tertiary dentin, their number and ability to produce dentin significantly decreases with age, posing a challenge to regenerative dentistry. If the primary odontoblasts are lost, pulp-derived

mesenchymal cells are induced to differentiate into odontoblast-like cells, forming reparative dentin. DPSC have previously been shown to successfully differentiate towards osteogenic and odontogenic fates[23-25] and have been characterized in detail[26]. Unfortunately DPSC expansion and regeneration capacity is limited[27], showing a dramatic decrease in regenerative capacity with increased age[28]. Thus, the iOB protocol described here provides a model essential to study genetic diseases affecting dentin formation, interlayer communication involved in odontogenesis, as well as regeneration of tooth dentin structure.

Odontoblasts are believed to develop through reciprocal, repeated signaling interactions with the dental epithelium derived ameloblasts. Our signaling pathway analysis indicates that the majority of signaling ligands critical for odontoblast development are produced by the dental epithelium derived inner enamel epithelium and pre-ameloblast at early and late tooth development, respectively. Interestingly, the bulk of BMP signaling ligands received by the POB as it transitions to OB are secreted by the SOB, indicating a supportive role for this novel cell type in human OB development. While previous studies have focused on the role of a single signaling pathway, many others have highlighted the importance of crosstalk between pathways in tooth development and maintenance[131-133]. Our predictive pathway analysis highlights not only the primary pathway responsible for each stage, but ranks the other pathways involved, meaning that our study will facilitate the investigation into both previously identified and yet undescribed crosstalks in driving forward development. The detailed analysis we have provided in this study will facilitate more detailed and informed studies on degenerative dental diseases and can lead to the development of more effective

ways to mitigate or reverse tooth loss. Furthermore, our work with AI-designed, de novo receptor mini-binders that specifically bind and either activate or inhibit target receptor signaling[134,135] now reveals a novel, highly simplified method to identify the exact stage-specific signaling pathway required in the differentiation process. The method described in this study using the de novo FGFR-minibinder to unravel the FGFR pathway requirement in odontoblast maturation will be generally applicable and specific to any signaling pathway analyzed in differentiation of normal and disease organoids.

Future studies focused on co-culture of the iOB described here with our lab's HiPSC-derived ameloblasts (iAM)[136] will provide an unprecedented tool for studying the signaling patterns exchanged between these tissue types during tooth development, likely resulting in further maturation of both cell types.

Though DLX3 has been shown to be expressed in murine neural crest cells, our study illustrates this transcription factor is not required for differentiation of human induced pluripotent stem cells to neural crest fate. Our findings support previous murine models indicating loss of DLX3 results in downregulated expression of odontoblast marker DSPP. Further, we show that DLX3 mutants have inhibited mineralization capacity, indicating odontoblast maturity is arrested by loss of this transcription factor. Importantly, our findings indicate that loss of DLX3 impacts odontoblast development at the POB stage, deepening our understanding of DLX3's role in human odontoblast development and taking the field one step closer to developing therapies for Tricho-Dento-Osseous Syndrome.

The overall significance of this study is threefold: 1) providing unprecedented insight at the single cell level into cell types of the developing tooth dental

ectomesenchyme; 2) applying the revealed molecular signaling that controls human odontoblast cell lineage commitment during differentiation to generate a HiPSC-derived odontoblast differentiation method (iOB); 3) utilizing the iOB tool to study the molecular mechanism of human odontoblast differentiation in states of health and disease in order to design appropriate therapies.

LITERATURE CITED

1. Zhang, Y., Wang, S., Song, Y., Han, J., Chai, Y., & Chen, Y. (2003). Timing of odontogenic neural crest cell migration and tooth-forming capability in mice. *Developmental dynamics: an official publication of the American Association of Anatomists*, *226*(4), 713-718.
2. Osumi-Yamashita, N., Ninomiya, Y., Eto, K., & Doi, H. (1994). The contribution of both forebrain and midbrain crest cells to the mesenchyme in the frontonasal mass of mouse embryos. *Developmental biology*, *164*(2), 409-419.
3. Chai, Y., Jiang, X., Ito, Y., Bringas, P., Han, J., Rowitch, D. H., ... & Sucov, H. M. (2000). Fate of the mammalian cranial neural crest during tooth and mandibular morphogenesis. *Development*, *127*(8), 1671-1679.
4. Goldberg, M., & Smith, A. J. (2004). Cells and extracellular matrices of dentin and pulp: a biological basis for repair and tissue engineering. *Critical Reviews in Oral Biology & Medicine*, *15*(1), 13-27.
5. Harada, M., Kenmotsu, S. I., Nakasone, N., Nakakura-Ohshima, K., & Ohshima, H. (2008). Cell dynamics in the pulpal healing process following cavity preparation in rat molars. *Histochemistry and Cell Biology*, *130*(4), 773-783.
6. Hosoya, A., Hiraga, T., Ninomiya, T., Yukita, A., Yoshiba, K., Yoshiba, N., ... & Nakamura, H. (2012). Thy-1-positive cells in the subodontoblastic layer possess high potential to differentiate into hard tissue-forming cells. *Histochemistry and cell biology*, *137*(6), 733-742.
7. Zhao, H., Feng, J., Seidel, K., Shi, S., Klein, O., Sharpe, P., & Chai, Y. (2014). Secretion of shh by a neurovascular bundle niche supports mesenchymal stem cell homeostasis in the adult mouse incisor. *Cell stem cell*, *14*(2), 160-173.
8. Kaukua, N., Shahidi, M. K., Konstantinidou, C., Dyachuk, V., Kaucka, M., Furlan, A., ... & Adameyko, I. (2014). Glial origin of mesenchymal stem cells in a tooth model system. *Nature*, *513*(7519), 551-554.
9. Seidel, K., Marangoni, P., Tang, C., Houshmand, B., Du, W., Maas, R. L., ... & Klein, O. D. (2017). Resolving stem and progenitor cells in the adult mouse incisor through gene co-expression analysis. *Elife*, *6*, e24712.
10. Oxilia, G., Fiorillo, F., Boschin, F., Boaretto, E., Apicella, S. A., Matteucci, C., ... & Benazzi, S. (2017). The dawn of dentistry in the late upper Paleolithic: An early case of pathological intervention at Riparo Fredian. *American journal of physical anthropology*, *163*(3), 446-461.
11. MeatScepterGuy. (2022). If you had the ability to add a feature to the human body, what would it be? *Online forum post.* https://www.reddit.com/r/AskReddit/comments/ukx8w1/if_you_had_the_ability_to_add_a_feature_to_the/
12. James, S. L., Abate, D., Abate, K. H., Abay, S. M., Abbafati, C., Abbasi, N., ... & Briggs, A. M. (2018). Global, regional, and national incidence, prevalence, and

years lived with disability for 354 diseases and injuries for 195 countries and territories, 1990–2017: a systematic analysis for the Global Burden of Disease Study 2017. *The Lancet*, *392*(10159), 1789-1858.
13. Centers for Disease Control and Prevention. (2019) Oral Health Surveillance Report: Trends in Dental Caries and Sealants, Tooth Retention, and Edentulism, United States, 1999–2004 to 2011–2016.
14. Nalliah, R. P., Allareddy, V., Elangovan, S., Karimbux, N., Lee, M. K., Gajendrareddy, P., & Allareddy, V. (2011). Hospital emergency department visits attributed to pulpal and periapical disease in the United States in 2006. *Journal of endodontics*, *37*(1), 6-9.
15. Henry, D. B. (2009). The consequences of restorative cycles. *Operative Dentistry*, *34*(6), 759-760.
16. Derks, J., Schaller, D., Håkansson, J., Wennström, J. L., Tomasi, C., & Berglundh, T. (2016). Effectiveness of implant therapy analyzed in a Swedish population: prevalence of peri-implantitis. *Journal of dental research*, *95*(1), 43-49.
17. Zander, H. A. (1939). Reaction of the pulp to calcium hydroxide. *Journal of Dental Research*, *18*(4), 373-379.
18. Doyle, T. L., Casas, M. J., Kenny, D. J., & Judd, P. L. (2010). Mineral trioxide aggregate produces superior outcomes in vital primary molar pulpotomy. *Pediatric dentistry*, *32*(1), 41-47.
19. Maturo, P., Costacurta, M., Bartolino, M., & Docimo, R. (2009). MTA applications in pediatric dentistry. *Oral & implantology*, *2*(3), 37.
20. Nowicka, A., Lipski, M., Parafiniuk, M., Sporniak-Tutak, K., Lichota, D., Kosierkiewicz, A., ... & Buczkowska-Radlińska, J. (2013). Response of human dental pulp capped with biodentine and mineral trioxide aggregate. *Journal of endodontics*, *39*(6), 743-747.
21. Neves, V., Babb, R., Chandrasekaran, D., & Sharpe, P. T. (2017). Promotion of natural tooth repair by small molecule GSK3 antagonists. *Scientific reports*, *7*(1), 1-7.
22. Smith, A, Sharpe, P. (2014). Biological Tooth Replacement and Repair. Principles of Tissue Engineering, 1471-1485.
23. Gronthos, S., Mankani, M., Brahim, J., Robey, P. G., & Shi, S. (2000). Postnatal human dental pulp stem cells (DPSCs) in vitro and in vivo. *Proceedings of the National Academy of Sciences*, *97*(25), 13625-13630.
24. Suzuki, T., Lee, C. H., Chen, M., Zhao, W., Fu, S. Y., Qi, J. J., ... & Mao, J. J. (2011). Induced migration of dental pulp stem cells for in vivo pulp regeneration. *Journal of dental research*, *90*(8), 1013-1018.

25. Kim, S. G., Zheng, Y., Zhou, J., Chen, M., Embree, M. C., Song, K., ... & Mao, J. J. (2013). Dentin and dental pulp regeneration by the patient's endogenous cells. *Endodontic topics*, *28*(1), 106-117.
26. Macrin, D., Alghadeer, A., Zhao, Y. T., Miklas, J. W., Hussein, A. M., Detraux, D., ... & Ruohola-Baker, H. (2019). Metabolism as an early predictor of DPSCs aging. *Scientific reports*, *9*(1), 1-19.
27. Mehrazarin, S., Oh, J. E., Chung, C. L., Chen, W., Kim, R. H., Shi, S., ... & Kang, M. K. (2011). Impaired odontogenic differentiation of senescent dental mesenchymal stem cells is associated with loss of Bmi-1 expression. *Journal of endodontics*, *37*(5), 662-666.
28. Iohara, K., Murakami, M., Nakata, K., & Nakashima, M. (2014). Age-dependent decline in dental pulp regeneration after pulpectomy in dogs. *Experimental Gerontology*, *52*, 39-45.
29. Sonoyama, W., Liu, Y., Yamaza, T., Tuan, R. S., Wang, S., Shi, S., & Huang, G. T. J. (2008). Characterization of the apical papilla and its residing stem cells from human immature permanent teeth: a pilot study. *Journal of endodontics*, *34*(2), 166-171.
30. Bakopoulou, A., Leyhausen, G., Volk, J., Tsiftsoglou, A., Garefis, P., Koidis, P., & Geurtsen, W. (2011). Comparative analysis of in vitro osteo/odontogenic differentiation potential of human dental pulp stem cells (DPSCs) and stem cells from the apical papilla (SCAP). *Archives of oral biology*, *56*(7), 709-721.
31. He, X. T., Wu, R. X., & Chen, F. M. (2020). Periodontal tissue engineering and regeneration. In *Principles of Tissue Engineering* (pp. 1221-1249). Academic Press.
32. Takahashi, K., & Yamanaka, S. (2006). Induction of pluripotent stem cells from mouse embryonic and adult fibroblast cultures by defined factors. *cell*, *126*(4), 663-676.
33. Young, C. S., Terada, S., Vacanti, J. P., Honda, M., Bartlett, J. D., & Yelick, P. C. (2002). Tissue engineering of complex tooth structures on biodegradable polymer scaffolds. *Journal of dental research*, *81*(10), 695-700.
34. Duailibi, M. T., Duailibi, S. E., Young, C. S., Bartlett, J. D., Vacanti, J. P., & Yelick, P. C. (2004). Bioengineered teeth from cultured rat tooth bud cells. *Journal of dental research*, *83*(7), 523-528.
35. Young, C. S., Kim, S. W., Qin, C., Baba, O., Butler, W. T., Taylor, R. R., ... & Yelick, P. C. (2005). Developmental analysis and computer modelling of bioengineered teeth. *Archives of Oral Biology*, *50*(2), 259-265.
36. Yang, X., Yang, F., Walboomers, X. F., Bian, Z., Fan, M., & Jansen, J. A. (2010). The performance of dental pulp stem cells on nanofibrous PCL/gelatin/nHA scaffolds. *Journal of Biomedical Materials Research Part A: An Official Journal of The Society for Biomaterials, The Japanese Society for Biomaterials, and The*

Australian Society for Biomaterials and the Korean Society for Biomaterials, *93*(1), 247-257.
37. Banchs, F., & Trope, M. (2004). Revascularization of immature permanent teeth with apical periodontitis: new treatment protocol?. *Journal of endodontics*, *30*(4), 196-200.
38. Zhao, Y. T., Fallas, J. A., Saini, S., Ueda, G., Somasundaram, L., Zhou, Z., ... & Ruohola-Baker, H. (2021). F-domain valency determines outcome of signaling through the angiopoietin pathway. *EMBO reports*, *22*(12), e53471.
39. Divine, R., Dang, H. V., Ueda, G., Fallas, J. A., Vulovic, I., Sheffler, W., ... & Baker, D. (2021). Designed proteins assemble antibodies into modular nanocages. *Science*, *372*(6537), eabd9994.
40. Ben-Sasson, A. J., Watson, J. L., Sheffler, W., Johnson, M. C., Bittleston, A., Somasundaram, L., ... & Baker, D. (2021). Design of biologically active binary protein 2D materials. *Nature*, *589*(7842), 468-473.
41. Jussila, M., & Thesleff, I. (2012). Signaling networks regulating tooth organogenesis and regeneration, and the specification of dental mesenchymal and epithelial cell lineages. *Cold Spring Harbor perspectives in biology*, *4*(4), a008425.
42. Nanci, A. (2017). *Ten Cate's Oral Histology-e-book: development, structure, and function*. Elsevier Health Sciences.
43. Thesleff, I., & Sharpe, P. (1997). Signalling networks regulating dental development. *Mechanisms of development*, *67*(2), 111-123.
44. Bei, M., Kratochwil, K., & Maas, R. L. (2000). BMP4 rescues a non-cell-autonomous function of Msx1 in tooth development. *Development*, *127*(21), 4711-4718.
45. Ohuchi, H., Hori, Y., Yamasaki, M., Harada, H., Sekine, K., Kato, S., & Itoh, N. (2000). FGF10 acts as a major ligand for FGF receptor 2 IIIb in mouse multi-organ development. *Biochemical and biophysical research communications*, *277*(3), 643-649.
46. De Moerlooze, L., Spencer-Dene, B., Revest, J., Hajihosseini, M., Rosewell, I., & Dickson, C. (2000). An important role for the IIIb isoform of fibroblast growth factor receptor 2 (FGFR2) in mesenchymal-epithelial signalling during mouse organogenesis. *Development*, *127*(3), 483-492.
47. Jernvall, J., Kettunen, P., Karavanova, I., Martin, L. B., & Thesleff, I. (2002). Evidence for the role of the enamel knot as a control center in mammalian tooth cusp formation: non-dividing cells express growth stimulating Fgf-4 gene. *International Journal of Developmental Biology*, *38*(3), 463-469.
48. Huang, F., Hu, X., Fang, C., Liu, H., Lin, C., Zhang, Y., & Hu, X. (2015). Expression profile of critical genes involved in FGF signaling pathway in the

developing human primary dentition. *Histochemistry and cell biology*, *144*(5), 457-469.
49. Dassule, H. R., Lewis, P., Bei, M., Maas, R., & McMahon, A. P. (2000). Sonic hedgehog regulates growth and morphogenesis of the tooth. *Development*, *127*(22), 4775-4785.
50. Ishikawa, Y., Ida-Yonemochi, H., Saito, K., Nakatomi, M., & Ohshima, H. (2021). The Sonic hedgehog–Patched–Gli signaling pathway maintains dental epithelial and pulp stem/progenitor cells and regulates the function of odontoblasts. *Frontiers in Dental Medicine*, *2*, 651334.
51. Kolodziejczyk, A. A., Kim, J. K., Svensson, V., Marioni, J. C., & Teichmann, S. A. (2015). The technology and biology of single-cell RNA sequencing. *Molecular cell*, *58*(4), 610-620.
52. Pagella, P., de Vargas Roditi, L., Stadlinger, B., Moor, A. E., & Mitsiadis, T. A. (2021). A single-cell atlas of human teeth. *IScience*, *24*(5), 102405.
53. Krivanek, J., Soldatov, R. A., Kastriti, M. E., Chontorotzea, T., Herdina, A. N., Petersen, J., ... & Adameyko, I. (2020). Dental cell type atlas reveals stem and differentiated cell types in mouse and human teeth. *Nature communications*, *11*(1), 1-18.
54. Chiba, Y., Saito, K., Martin, D., Boger, E. T., Rhodes, C., Yoshizaki, K., ... & Fukumoto, S. (2020). Single-cell RNA-sequencing from mouse incisor reveals dental epithelial cell-type specific genes. *Frontiers in cell and developmental biology*, *8*, 841.
55. Otsu, K., Kishigami, R., Oikawa-Sasaki, A., Fukumoto, S., Yamada, A., Fujiwara, N., ... & Harada, H. (2012). Differentiation of induced pluripotent stem cells into dental mesenchymal cells. *Stem cells and development*, *21*(7), 1156-1164.
56. Kim, E. J., Yoon, K. S., Arakaki, M., Otsu, K., Fukumoto, S., Harada, H., ... & Jung, H. S. (2019). Effective differentiation of induced pluripotent stem cells into dental cells. *Developmental Dynamics*, *248*(1), 129-139.
57. Seki, D., Takeshita, N., Oyanagi, T., Sasaki, S., Takano, I., Hasegawa, M., & Takano-Yamamoto, T. (2015). Differentiation of odontoblast-like cells from mouse induced pluripotent stem cells by Pax9 and Bmp4 transfection. *Stem Cells Translational Medicine*, *4*(9), 993-997.
58. Takada, K., Odashima, A., Onodera, S., Saito, A., Aida, N., Furusawa, M., & Azuma, T. (2022). The effect of BMP4, FGF8 and WNT3a on mouse iPS cells differentiating to odontoblast-like cells. *Medical Molecular Morphology*, 1-11.
59. Xie, H., Dubey, N., Shim, W., Ramachandra, C. J., Min, K. S., Cao, T., & Rosa, V. I. N. I. C. I. U. S. (2018). Functional odontoblastic-like cells derived from human iPSCs. *Journal of Dental Research*, *97*(1), 77-83.
60. Dong, J., Amor, D., Aldred, M. J., Gu, T., Escamilla, M., & MacDougall, M. (2005). DLX3 mutation associated with autosomal dominant amelogenesis imperfecta

with taurodontism. *American Journal of Medical Genetics Part A*, *133*(2), 138-141.
61. Price, J. A., Bowden, D. W., Tim Wright, J., Pettenati, M. J., & Hart, T. C. (1998). Identification of a mutation in DLX3 associated with tricho-dento-osseous (TDO) syndrome. *Human molecular genetics*, *7*(3), 563-569.
62. Nieminen, P., Lukinmaa, P. L., Alapulli, H., Methuen, M., Suojärvi, T., Kivirikko, S., ... & Alaluusua, S. (2011). DLX3 homeodomain mutations cause tricho-dento-osseous syndrome with novel phenotypes. *Cells Tissues Organs*, *194*(1), 49-59.
63. Robinson, G. W., & Mahon, K. A. (1994). Differential and overlapping expression domains of Dlx-2 and Dlx-3 suggest distinct roles for Distal-less homeobox genes in craniofacial development. *Mechanisms of development*, *48*(3), 199-215.
64. Duverger, O., Zah, A., Isaac, J., Sun, H. W., Bartels, A. K., Lian, J. B., ... & Morasso, M. I. (2012). Neural crest deletion of Dlx3 leads to major dentin defects through down-regulation of Dspp. *Journal of Biological Chemistry*, *287*(15), 12230-12240.
65. Choi, S. J., Song, I. S., Feng, J. Q., Gao, T., Haruyama, N., Gautam, P., ... & Hart, T. C. (2010). Mutant DLX 3 disrupts odontoblast polarization and dentin formation. *Developmental biology*, *344*(2), 682-692.
66. Zhan, Y., Li, X., Gou, X., Yuan, G., Fan, M., & Yang, G. (2018). DLX3 inhibits the proliferation of human dental pulp cells through inactivation of canonical Wnt/β-catenin signaling pathway. *Frontiers in physiology*, *9*, 1637.
67. Nelson, S. J. (2014). *Wheeler's dental anatomy, physiology and occlusion-e-book*. Elsevier Health Sciences.
68. Cao, J., Spielmann, M., Qiu, X., Huang, X., Ibrahim, D. M., Hill, A. J., ... & Shendure, J. (2019). The single-cell transcriptional landscape of mammalian organogenesis. *Nature*, *566*(7745), 496-502.
69. Trapnell, C., Cacchiarelli, D., Grimsby, J., Pokharel, P., Li, S., Morse, M., ... & Rinn, J. L. (2014). The dynamics and regulators of cell fate decisions are revealed by pseudotemporal ordering of single cells. *Nature biotechnology*, *32*(4), 381-386.
70. Qiu, X., Mao, Q., Tang, Y., Wang, L., Chawla, R., Pliner, H. A., & Trapnell, C. (2017). Reversed graph embedding resolves complex single-cell trajectories. *Nature methods*, *14*(10), 979-982.
71. McInnes, L., Healy, J., & Melville, J. (2018). Umap: Uniform manifold approximation and projection for dimension reduction. *arXiv preprint arXiv:1802.03426*.
72. Balic, A., & Thesleff, I. (2015). Tissue interactions regulating tooth development and renewal. *Current topics in developmental biology*, *115*, 157-186.

73. Mucchielli, M. L., Mitsiadis, T. A., Raffo, S., Brunet, J. F., Proust, J. P., & Goridis, C. (1997). MouseOtlx2/RIEGExpression in the odontogenic epithelium precedes tooth initiation and requires mesenchyme-derived signals for its maintenance. *Developmental biology*, *189*(2), 275-284.
74. Balic, A., Adams, D., & Mina, M. (2009). Prx1 and Prx2 cooperatively regulate the morphogenesis of the medial region of the mandibular process. *Developmental dynamics: an official publication of the American Association of Anatomists*, *238*(10), 2599-2613.
75. Åberg, T., Wang, X. P., Kim, J. H., Yamashiro, T., Bei, M., Rice, R., ... & Thesleff, I. (2004). Runx2 mediates FGF signaling from epithelium to mesenchyme during tooth morphogenesis. *Developmental biology*, *270*(1), 76-93.
76. Gu, Z., Eils, R., & Schlesner, M. (2016). Complex heatmaps reveal patterns and correlations in multidimensional genomic data. *Bioinformatics*, *32*(18), 2847-2849.
77. Brionne, A., Juanchich, A., & Hennequet-Antier, C. (2019). ViSEAGO: a Bioconductor package for clustering biological functions using Gene Ontology and semantic similarity. *BioData mining*, *12*(1), 1-13.
78. Gu, Z., & Hübschmann, D. (2022). Simplify enrichment: A bioconductor package for clustering and visualizing functional enrichment results. *Genomics, Proteomics & Bioinformatics*.
79. Butler, A., Hoffman, P., Smibert, P., Papalexi, E., & Satija, R. (2018). Integrating single-cell transcriptomic data across different conditions, technologies, and species. *Nature biotechnology*, *36*(5), 411-420.
80. Sharir, A., Marangoni, P., Zilionis, R., Wan, M., Wald, T., Hu, J. K., ... & Klein, O. D. (2019). A large pool of actively cycling progenitors orchestrates self-renewal and injury repair of an ectodermal appendage. *Nature cell biology*, *21*(9), 1102-1112.
81. Weinreb, C., Wolock, S., & Klein, A. M. (2018). SPRING: a kinetic interface for visualizing high dimensional single-cell expression data. *Bioinformatics*, *34*(7), 1246-1248.
82. Wang, Y. (2020). talklr uncovers ligand-receptor mediated intercellular crosstalk. *BioRxiv*.
83. Miao, Z., Deng, K., Wang, X., & Zhang, X. (2018). DEsingle for detecting three types of differential expression in single-cell RNA-seq data. *Bioinformatics*, *34*(18), 3223-3224.
84. Wang, F., Flanagan, J., Su, N., Wang, L. C., Bui, S., Nielson, A., ... & Luo, Y. (2012). RNAscope: a novel in situ RNA analysis platform for formalin-fixed, paraffin-embedded tissues. *The Journal of molecular diagnostics*, *14*(1), 22-29.

85. Bankhead, P., Loughrey, M. B., Fernández, J. A., Dombrowski, Y., McArt, D. G., Dunne, P. D., ... & Hamilton, P. W. (2017). QuPath: Open source software for digital pathology image analysis. *Scientific reports*, *7*(1), 1-7.
86. Schindelin, J., Arganda-Carreras, I., Frise, E., Kaynig, V., Longair, M., Pietzsch, T., ... & Cardona, A. (2012). Fiji: an open-source platform for biological-image analysis. *Nature methods*, *9*(7), 676-682.
87. Schindelin, J., Rueden, C. T., Hiner, M. C., & Eliceiri, K. W. (2015). The ImageJ ecosystem: An open platform for biomedical image analysis. *Molecular reproduction and development*, *82*(7-8), 518-529.
88. Miyaoka, Y., Chan, A. H., Judge, L. M., Yoo, J., Huang, M., Nguyen, T. D., ... & Conklin, B. R. (2014). Isolation of single-base genome-edited human iPS cells without antibiotic selection. *Nature methods*, *11*(3), 291-293.
89. Mandegar, M. A., Huebsch, N., Frolov, E. B., Shin, E., Truong, A., Olvera, M. P., ... & Conklin, B. R. (2016). CRISPR interference efficiently induces specific and reversible gene silencing in human iPSCs. *Cell stem cell*, *18*(4), 541-553.
90. Ferreccio, A., Mathieu, J., Detraux, D., Somasundaram, L., Cavanaugh, C., Sopher, B., ... & Ruohola-Baker, H. (2018). Inducible CRISPR genome editing platform in naive human embryonic stem cells reveals JARID2 function in self-renewal. *Cell Cycle*, *17*(5), 535-549.
91. Chen, G., Gulbranson, D. R., Hou, Z., Bolin, J. M., Ruotti, V., Probasco, M. D., ... & Thomson, J. A. (2011). Chemically defined conditions for human iPSC derivation and culture. *Nature methods*, *8*(5), 424-429.
92. Chambers, S. M., Fasano, C. A., Papapetrou, E. P., Tomishima, M., Sadelain, M., & Studer, L. (2009). Highly efficient neural conversion of human ES and iPS cells by dual inhibition of SMAD signaling. *Nature biotechnology*, *27*(3), 275-280.
93. Flanagan, M., Gimble, J. M., Yu, G., Wu, X., Xia, X., Hu, J., ... & Li, S. (2011). Competitive electroporation formulation for cell therapy. *Cancer gene therapy*, *18*(8), 579-586.
94. de Paula, F., Teshima, T. H. N., Hsieh, R., Souza, M. M., Nico, M. M. S., & Lourenco, S. V. (2017). Overview of human salivary glands: highlights of morphology and developing processes. *The Anatomical Record*, *300*(7), 1180-1188.
95. Radlanski, R. J., Renz, H., Zimmermann, C. A., Schuster, F. P., Voigt, A., & Heikinheimo, K. (2016). Chondral ossification centers next to dental primordia in the human mandible: a study of the prenatal development ranging between 68 to 270 mm CRL. *Annals of Anatomy-Anatomischer Anzeiger*, *208*, 49-57.
96. Wise, G. E., Marks Jr, S. C., & Zhao, L. (1998). Effect of CSF-1 on in vivo expression of c-fos in the dental follicle during tooth eruption. *European Journal of Oral Sciences*, *106*(S1), 397-400.

97. Kardos, T. B., & Hubbard, M. J. (1981). Rapid dissection of rodent molar-tooth germs. *Laboratory animals*, *15*(4), 371-373.
98. Cha, S. (Ed.). (2017). *Salivary gland development and regeneration: Advances in research and clinical approaches to functional restoration*. Springer.
99. Quirós-Terrón, L., Arráez-Aybar, L. A., Murillo-González, J., De-la-Cuadra-Blanco, C., Martínez-Álvarez, M. C., Sanz-Casado, J. V., & Mérida-Velasco, J. R. (2019). Initial stages of development of the submandibular gland (human embryos at 5.5–8 weeks of development). *Journal of Anatomy*, *234*(5), 700-708.
100. Franzén, O., Gan, L. M., & Björkegren, J. L. (2019). PanglaoDB: a web server for exploration of mouse and human single-cell RNA sequencing data. *Database*, *2019*.
101. Albelda, S. M., Muller, W. A., Buck, C. A., & Newman, P. J. (1991). Molecular and cellular properties of PECAM-1 (endoCAM/CD31): a novel vascular cell-cell adhesion molecule. *The Journal of cell biology*, *114*(5), 1059-1068.
102. Jiang, L., Lin, L., Li, R., Yuan, C., Xu, M., Huang, J. H., & Huang, M. (2016). Dimer conformation of soluble PECAM-1, an endothelial marker. *The international journal of biochemistry & cell biology*, *77*, 102-108.
103. Lampugnani, M. G., Resnati, M., Raiteri, M., Pigott, R., Pisacane, A., Houen, G., ... & Dejana, E. (1992). A novel endothelial-specific membrane protein is a marker of cell-cell contacts. *The Journal of cell biology*, *118*(6), 1511-1522.
104. Böheim, K., Denz, H., Böheim, C., Glassl, H., & Huber, H. (1987). An immunohistologic study of the distribution and status of activation of head and neck tumor infiltrating leukocytes. *Archives of oto-rhino-laryngology*, *244*(2), 127-132.
105. Filion, L. G., Izaguirre, C. A., Garber, G. E., Huebsh, L., & Aye, M. T. (1990). Detection of surface and cytoplasmic CD4 on blood monocytes from normal and HIV-1 infected individuals. *Journal of immunological methods*, *135*(1-2), 59-69.
106. Ehnes, D.D., Alghadeer, A., Hanson-Drury, S., Zhao Y.T., Tilmes G., Mathieu J., Ruohola-Baker H. (In press). Sci-Seq of human fetal salivary tissue introduces human transcriptional paradigms and a novel cell population. *Frontiers in Dental Medicine.*
107. Mitchell, J. M., Hicklin, D. M., Doughty, P. M., Hicklin, J. H., Dickert Jr, J. W., Tolbert, S. M., ... & Kern, M. (2006). The Prx1 homeobox gene is critical for molar tooth morphogenesis. *Journal of dental research*, *85*(10), 888-893.
108. Saito, K., & Ohshima, H. (2019). The putative role of insulin-like growth factor (IGF)-binding protein 5 independent of IGF in the maintenance of pulpal homeostasis in mice. *Regenerative Therapy*, *11*, 217-224.
109. Hemeryck, L., Hermans, F., Chappell, J., Kobayashi, H., Lambrechts, D., Lambrichts, I., ... & Vankelecom, H. (2022). Organoids from human tooth showing

epithelial stemness phenotype and differentiation potential. *Cellular and Molecular Life Sciences*, *79*(3), 1-23.
110. Lee, H. S., Lee, J., Kim, S. O., Song, J. S., Lee, J. H., Lee, S. I., ... & Choi, B. J. (2013). Comparative gene-expression analysis of the dental follicle and periodontal ligament in humans. *PloS one*, *8*(12), e84201.
111. Kawasaki, K., Kawasaki, M., Watanabe, M., Idrus, E., Nagai, T., Oommen, S., ... & Ohazama, A. (2015). Expression of Sox genes in tooth development. *The International journal of developmental biology*, *59*(10-12), 471.
112. Kettunen, P., Laurikkala, J., Itäranta, P., Vainio, S., Itoh, N., & Thesleff, I. (2000). Associations of FGF-3 and FGF-10 with signaling networks regulating tooth morphogenesis. *Developmental dynamics: an official publication of the American Association of Anatomists*, *219*(3), 322-332.
113. Kira-Tatsuoka, M., Oka, K., Tsuruga, E., Ozaki, M., & Sawa, Y. (2015). Immunohistochemical expression of fibrillin-1 and fibrillin-2 during tooth development. *Journal of Periodontal Research*, *50*(6), 714-720.
114. Kibe, K., Nakatomi, M., Kataoka, S., Toyono, T., & Seta, Y. (2018). Hey1 and Hey2 are differently expressed during mouse tooth development. *Gene Expression Patterns*, *27*, 99-105.
115. Hosoya, A., Hiraga, T., Ninomiya, T., Yukita, A., Yoshiba, K., Yoshiba, N., ... & Nakamura, H. (2012). Thy-1-positive cells in the subodontoblastic layer possess high potential to differentiate into hard tissue-forming cells. *Histochemistry and cell biology*, *137*(6), 733-742.
116. Tanabe, K., Yoshiba, K., Yoshiba, N., Iwaku, M., & Ozawa, H. (2002). Immunohistochemical study on pulpal response in rat molars after cavity preparation by Er: YAG laser. *European journal of oral sciences*, *110*(3), 237-245.
117. Chen, S., Rani, S., Wu, Y., Unterbrink, A., Gu, T. T., Gluhak-Heinrich, J., ... & MacDougall, M. (2005). Differential regulation of dentin sialophosphoprotein expression by Runx2 during odontoblast cytodifferentiation. *Journal of Biological Chemistry*, *280*(33), 29717-29727.
118. D'souza, R. N., Cavender, A., Sunavala, G., Alvarez, J., Ohshima, T., Kulkarni, A. B., & MacDougall, M. (1997). Gene expression patterns of murine dentin matrix protein 1 (Dmp1) and dentin sialophosphoprotein (DSPP) suggest distinct developmental functions in vivo. *Journal of Bone and Mineral Research*, *12*(12), 2040-2049.
119. D'Souza, R. N., Aberg, T., Gaikwad, J., Cavender, A., Owen, M., Karsenty, G., & Thesleff, I. (1999). Cbfa1 is required for epithelial-mesenchymal interactions regulating tooth development in mice. *Development*, *126*(13), 2911-2920.
120. Miyazaki, T., Kanatani, N., Rokutanda, S., Yoshida, C., Toyosawa, S., Nakamura, R., ... & Komori, T. (2008). Inhibition of the terminal differentiation of

odontoblasts and their transdifferentiation into osteoblasts in Runx2 transgenic mice. *Archives of histology and cytology*, *71*(2), 131-146.

121. Hackland, J. O., Frith, T. J., Thompson, O., Navarro, A. M., Garcia-Castro, M. I., Unger, C., & Andrews, P. W. (2017). Top-down inhibition of BMP signaling enables robust induction of hPSCs into neural crest in fully defined, xeno-free conditions. *Stem cell reports*, *9*(4), 1043-1052.
122. Itoh, N. (2016). FGF10: A multifunctional mesenchymal–epithelial signaling growth factor in development, health, and disease. *Cytokine & growth factor reviews*, *28*, 63-69.
123. Chimal-Monroy, J., Rodriguez-Leon, J., Montero, J. A., Ganan, Y., Macias, D., Merino, R., & Hurle, J. M. (2003). Analysis of the molecular cascade responsible for mesodermal limb chondrogenesis: Sox genes and BMP signaling. *Developmental biology*, *257*(2), 292-301.
124. Hojo, H., Ohba, S., Taniguchi, K., Shirai, M., Yano, F., Saito, T., ... & Chung, U. I. (2013). Hedgehog-Gli activators direct osteo-chondrogenic function of bone morphogenetic protein toward osteogenesis in the perichondrium. *Journal of Biological Chemistry*, *288*(14), 9924-9932.
125. Mansukhani, A., Ambrosetti, D., Holmes, G., Cornivelli, L., & Basilico, C. (2005). Sox2 induction by FGF and FGFR2 activating mutations inhibits Wnt signaling and osteoblast differentiation. *The Journal of cell biology*, *168*(7), 1065-1076.
126. Ramirez, F., & Sakai, L. Y. (2010). Biogenesis and function of fibrillin assemblies. *Cell and tissue research*, *339*(1), 71-82.
127. Suda, N. (2008). Comprehensive gene expression analysis in human periodontal ligaments of the mandibular third molars performing vertical movement and the maxillary second premolars with occlusal contact. *Orthodontics & craniofacial research*, *11*(1), 1-7.
128. Bach, L. A. (2018). 40 years of IGF1: IGF-binding proteins. *Journal of molecular endocrinology*, *61*(1), T11-T28.
129. Cobb, L. J., Salih, D. A., Gonzalez, I., Tripathi, G., Carter, E. J., Lovett, F., ... & Pell, J. M. (2004). Partitioning of IGFBP-5 actions in myogenesis: IGF-independent anti-apoptotic function. *Journal of cell science*, *117*(9), 1737-1746.
130. Sun, M., Long, J., Yi, Y., & Xia, W. (2017). Importin α-importin β complex mediated nuclear translocation of insulin-like growth factor binding protein-5. *Endocrine Journal*, EJ17-0156.
131. Malik, Z., Alexiou, M., Hallgrimsson, B., Economides, A. N., Luder, H. U., & Graf, D. (2018). Bone morphogenetic protein 2 coordinates early tooth mineralization. *Journal of Dental Research*, *97*(7), 835-843.

132. Yu, M., Wong, S. W., Han, D., & Cai, T. (2019). Genetic analysis: Wnt and other pathways in nonsyndromic tooth agenesis. *Oral diseases*, *25*(3), 646-651.
133. Omi, M., Kulkarni, A. K., Raichur, A., Fox, M., Uptergrove, A., Zhang, H., & Mishina, Y. (2020). BMP‐Smad signaling regulates postnatal crown dentinogenesis in mouse molar. *JBMR plus*, *4*(2), e10249.
134. Cao, L., Coventry, B., Goreshnik, I., Huang, B., Sheffler, W., Park, J. S., ... & Baker, D. (2022). Design of protein-binding proteins from the target structure alone. *Nature*, *605*(7910), 551-560.
135. Edman, N., Redler, R., Schlichthaerle, T., Phal, A., Srivatsan, S., Etemadi, A., An, S., Ehnes, D., Gordon, M., Praetorius, F., Li, Z., Bethel, N., Cao, L., Carter, L., Miranda, M., Favor, A., Trapnell, C., Shendure, J., Bhabha, G., Ekiert, D., Ruohola-Baker, H., Schlessinger, J., Baker, D. Manuscript in preparation. De novo design of modular cyclic protein scaffolds to investigate receptor clustering.
136. Alghadeer A., Hanson-Drury S., Ehnes D.D., Zhao Y.T., Patni AP., Phal A., Zhang H., Wang Y., Doherty D., Glass I., Shendure J., Baker D., Rieger MC., Mathieu J., Ruohola-Baker H. Manuscript received. Human iPSC Derived Enamel Organoid Guided by Single Cell Atlas of Human Tooth Development. *Cell Stem Cell*.

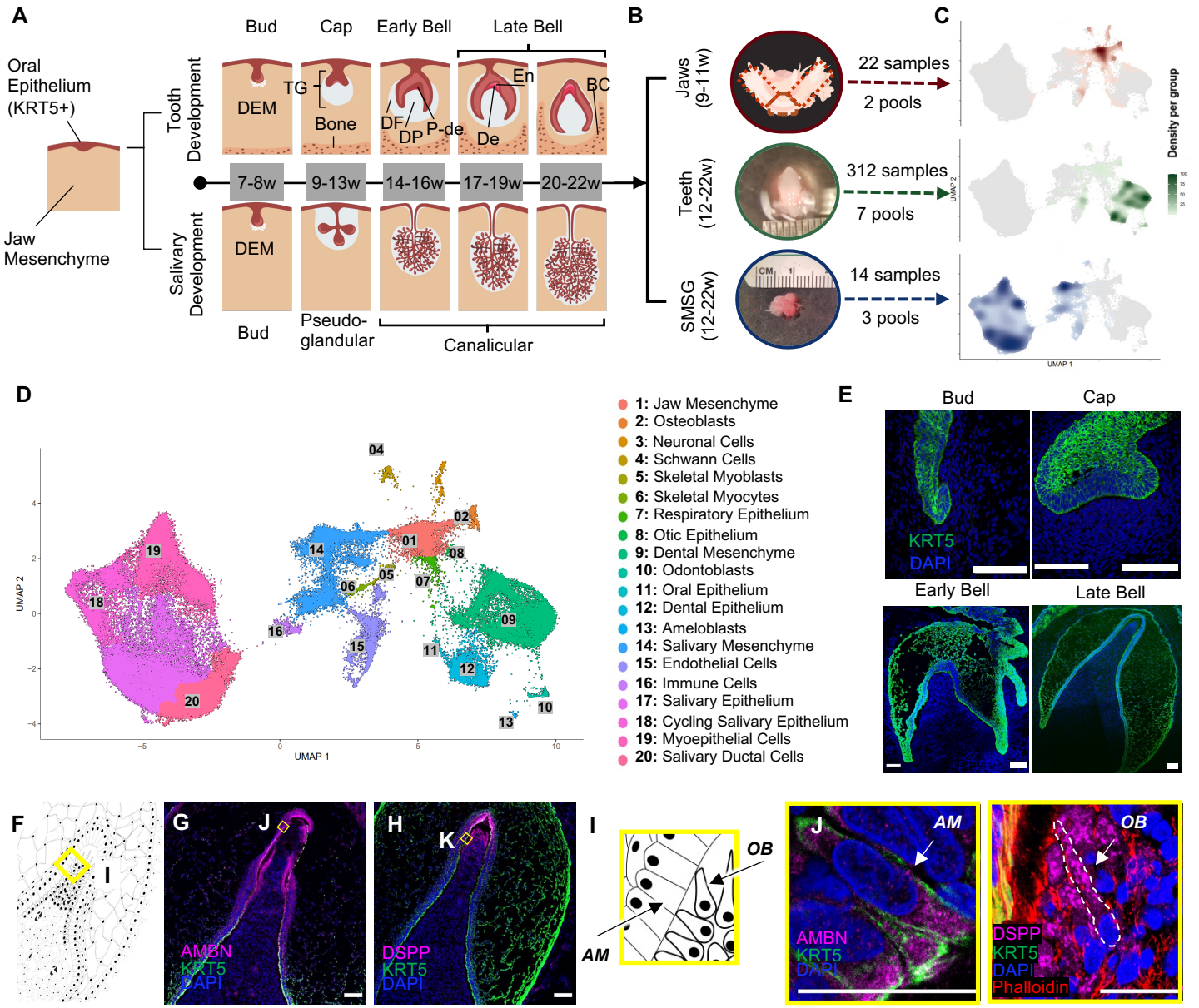

Figure 1. A single cell atlas of the developing human fetal jaws, teeth, and salivary glands tissues via sci-RNA-seq. Human tooth and salivary gland exhibit stepwise developmental processes (A). The oral epithelium (colored in red) will give rise to the epithelial components of teeth and salivary glands, while the condensed dental ectomesenchyme (DEM, colored in grey) will give rise to the mesenchymal component of these tissues. TG: toothgerm, DF: dental follicle, DP: dental papilla, P-de: pre-dentin, De: dentin, En: enamel matrix. (B) Human fetal tooth germs and salivary glands were dissected in a stage-specific manner from human fetal jaw tissue. The young fetal jaws, 9-11 gestational weeks were segmented into anterior segments (dotted box, which span from canine-to-canine region), and posterior jaw segment pairs (dotted box) and sequenced independently. For older fetal jaws, 12-22 gestational weeks, individual toothgerms and submandibular salivary glands were dissected (C) Density plots of the clustered sci-RNA-seq data highlight the location of each tissue type in the same UMAP coordinate in D. The UMAP graph (D) yielded 20 annotated clusters from all sequenced data. (E) Immunofluorescence staining of developing toothgerms tissue sections with anti-Krt5 (green) that specifically mark the dental epithelial morphology throughout the developmental stages. Counterstained with the nuclear staining DAPI (blue). To establish expression of known odontoblast and ameloblast markers in our tissue, immunohistochemistry was performed on human fetal toothgerm at 20gw using dentin sialophosphoprotein (DSPP) and ameloblastin (AMBN) respectively. As expected (Fig. 2B; S.Fig.1A), all oral epithelium derived tissue was visualized by KRT5 (green) (Fig. 1F-M), ameloblasts by AMBN (Fig.1F-I) (pink), and odontoblasts by DSPP (Fig.1J-M) (pink). We observe mirrored expression patterns of AMBN and DSPP between the ameloblast and odontoblast (Fig. 1G,H; Fig.3H,Q,Y) consistent with previous studies illustrating reciprocal expression between these two developing cell types. Scale bars: 50μm.

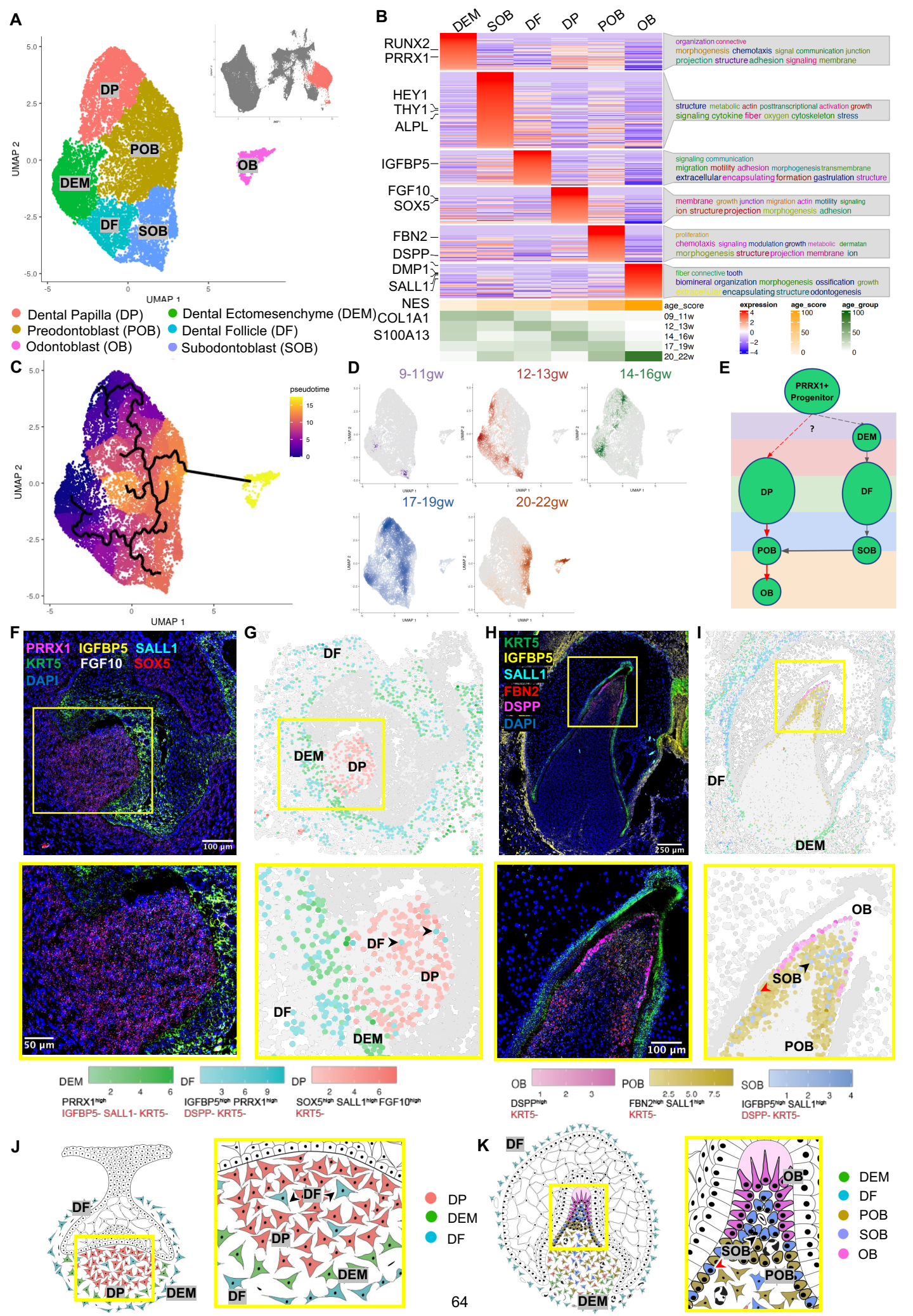
A
DP
POB
DEM
DF
SOB
OB
UMAP 1
UMAP 2
Dental Papilla (DP)
Preodontoblast (POB)
Odontoblast (OB)
Dental Ectomesenchyme (DEM)
Dental Follicle (DF)
Subodontoblast (SOB)
B
DEM SOB DF DP POB OB
RUNX2
PRRX1
HEY1
THY1
ALPL
IGFBP5
FGF10
SOX5
FBN2
DSPP
DMP1
SALL1
NES
COL1A1
S100A13
09_11w
12_13w
14_16w
17_19w
20_22w
age_score
expression
age_group
C
pseudotime
UMAP 1
UMAP 2
D
9-11gw
12-13gw
14-16gw
17-19gw
20-22gw
E
PRRX1+ Progenitor
?
DEM
DP
DF
POB
SOB
OB
F
PRRX1 IGFBP5 SALL1
KRT5 FGF10 SOX5
DAPI
100 μm
50 μm
G
DF
DEM
DP
H
KRT5
IGFBP5
SALL1
FBN2
DSPP
DAPI
250 μm
100 μm
I
DF
DEM
OB
SOB
POB
DEM PRRX1high IGFBP5- SALL1- KRT5-
DF IGFBP5high PRRX1high DSPP- KRT5-
DP SOX5high SALL1high FGF10high KRT5-
OB DSPPhigh KRT5-
POB FBN2high SALL1high KRT5-
SOB IGFBP5high SALL1high DSPP- KRT5-
J
DF
DP
DEM
DP
DEM
DF
K
DF
DEM
OB
SOB
POB
DEM
DF
POB
SOB
OB

Figure 2. Cell types identified by sciRNAseq are present at specific spatio-temporal stages of tooth development *in vivo*. (A) UMAP graph of subclustered molar and incisor tooth germ type dental mesenchyme derived cells from the total dataset identified 6 transcriptionally unique clusters including dental papilla (DP), preodontoblast (POB), odontoblast (OB), subodontoblast (SOB), odontoblast (OB), dental ectomesenchyme (DEM), and dental follicle (DF). (B) A custom heatmap was generated to identify the marker genes specific to each cluster, the top associated GO-terms to characterize cluster function, and calculated Age Score per cluster. (C) Pseudotime trajectory analysis for dental mesenchyme derived cells suggest two progenitors DP and DEM (blue), that give rise to differentiated OB (yellow). (D) Real-time density plots indicate migration of cells from early progenitor populations DEM and DP at 9-16gw to differentiated DF, POB, SOB and OB at later development 17-22gw. (E) Simplified differentiation trajectory tree illustrating a common PRRX1+ progenitor gives rise to both DP and DEM. In the OB lineage (red), DP gives rise to POB, followed by OB, with a suggested SOB transitioning through POB-like state before giving rise to OB; and DF lineage (grey), of DEM giving rise to DF. (F) RNAscope Multiplex in situ for DEM (PRRX1+), DP (SOX5+FGF10+SALL1+) and DF (IGFBP5+). (G) RNAscope map for marker combinations corresponding to individual dental mesenchyme clusters at 80d shown in aggregate in Figure 2F (black arrows indicate DF within the dental pulp). (H) RNAscope Multiplex in situ for OB (DSPP+), SOB (IGFBP5+SALL1+), POB (FBN2+SALL1+), and DF (IGFBP5+). (I) RNAscope map for marker combinations corresponding to individual dental mesenchyme clusters at 117d shown in aggregate in Figure 2H (SOB beneath OB at incisal edge (black arrow) and intermingled with POB (red arrow)). (J) A diagram of the developing dental mesenchyme derived cell types of the human tooth germ. At cap stage (12-13gw) the dental pulp consists of DP cells with DEM with sparse DF within; DF surrounds the developing toothgerm. (K) By bell stage (17-22gw), the dental pulp consists of OB at the incisal edge, SOB and POB with small contributions of the DEM and DP. Dental epithelium derived enamel organ is indicated by KRT5 (green, F and H; grey G and I).

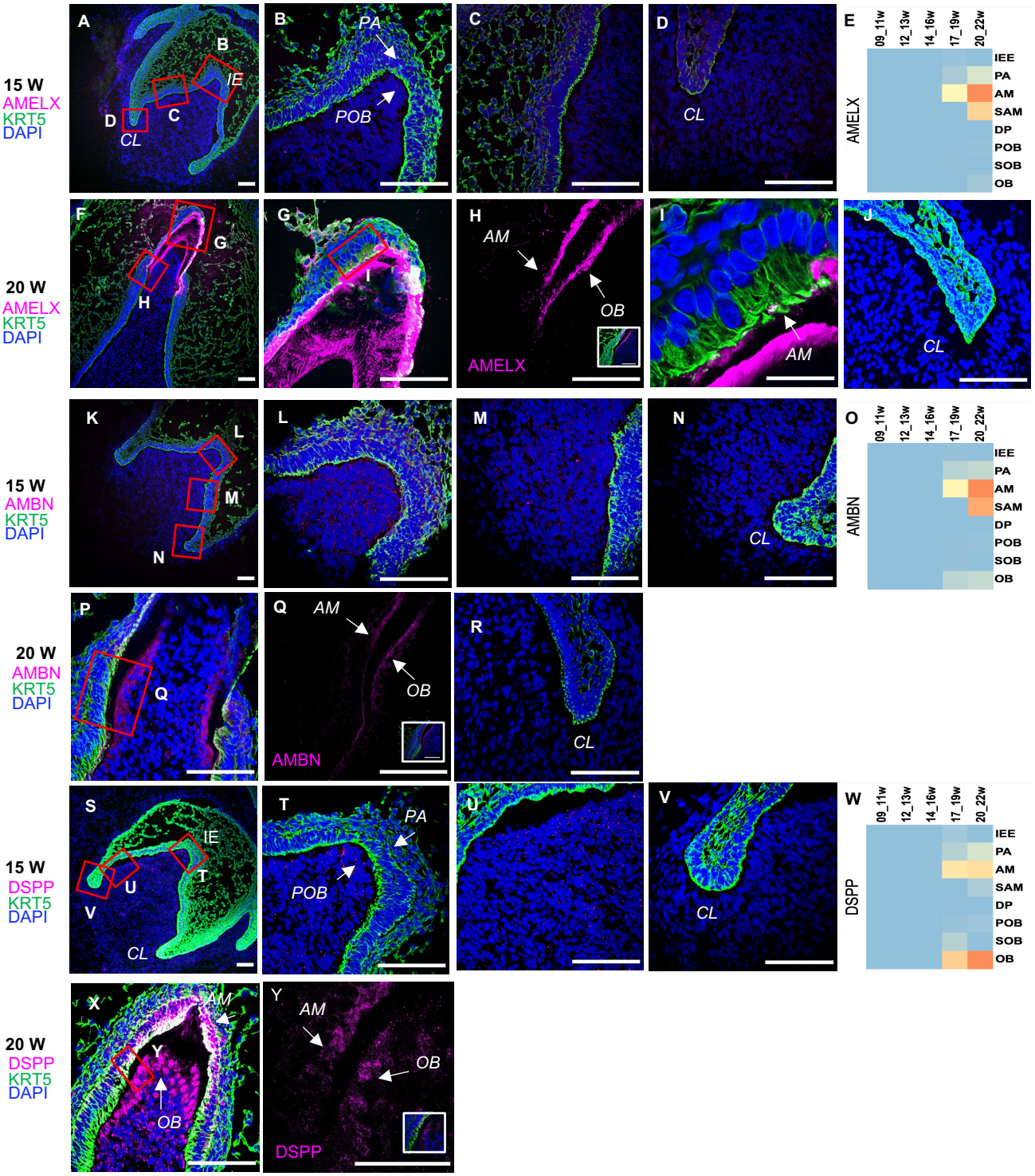

Figure 3. Spatial Expression of Odontoblast and Ameloblast Markers Differs Markedly from Early to Late Toothgerm Development. Ameloblast markers amelogenin (AMELX) and ameloblastin expression begins in the ameloblast after the early bell stage (A-J, K-R). Similarly, odontoblast marker dentin sialo phosphoprotein (DSPP) begins in the odontoblast after the early bell stage (S-Y). Heatmaps of expression over time of AMELX (E), AMBN (O), and DSPP (W). AMELX, AMBN and DSPP show mirrored expression patterns in ameloblasts and odontoblasts at late bell stage (H,Q,Y). Abbreviations: preodontoblast (POB), odontoblast (OB), preameloblast (PA) ameloblast (AM), incisal edge (IE), cervical loop (CL). Scale bars: 50μm.

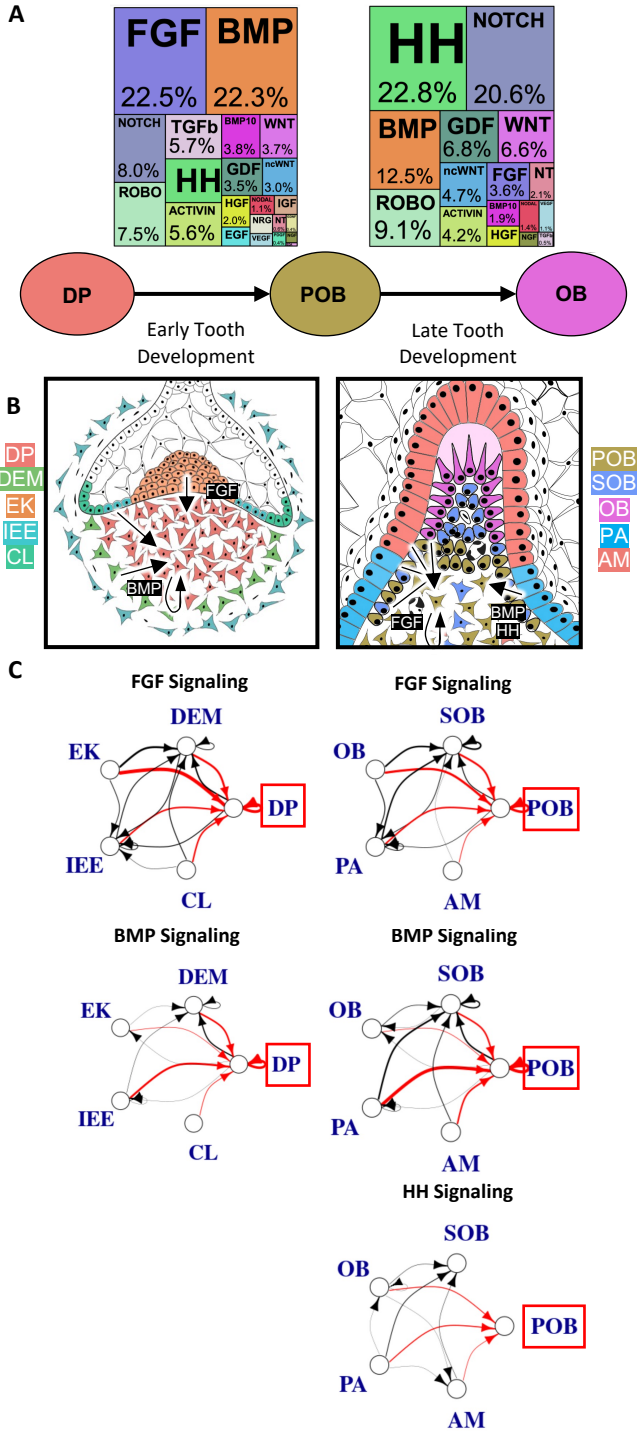

Figure 4. Top signaling pathways of odontoblast differentiation trajectory. (A) Downstream signaling pathways ranked by activity in odontoblast differentiation indicate FGF and BMP are critical to the DP as it transitions to POB; HH, BMP and NOTCH are the most active as POB transitions to OB. (B) Diagrams illustrate the dental epithelium and ectomesenchyme derived cells present during early tooth development (9-16gw) and late tooth development (17-22gw), and the suggested ligand sources for each pathway during the transition from DP to POB and POB to OB. Note that the far right image is an inset of the whole toothgerm focused on the incisal edge. The majority of FGF and BMP signaling ligands are produced by the dental epithelium derived EK and IEE, with BMP ligands also produced by the dental ectomesenchyme derived DEM and DP during the transition from DP to POB. During the transition from POB to OB, the dental epithelium derived PA and AM produce much of the FGF, BMP and HH signaling ligands; a smaller contribution of FGF ligands is made by the SOB and autocrine signaling from the POB. (C) The sources of critical signaling ligands for the top pathways involved for each developmental stage originate from both the dental epithelium and mesenchyme derived tissues, with the thickness of the line indicating the number of ligand: receptor interactions, arrowheads indicating the cell possessing the receptor, and interactions of interest (red) and between support cells (black). (D) Heatmaps for the top pathways were generated by aggregating pathway ligand gene expression, which is then averaged per cluster.

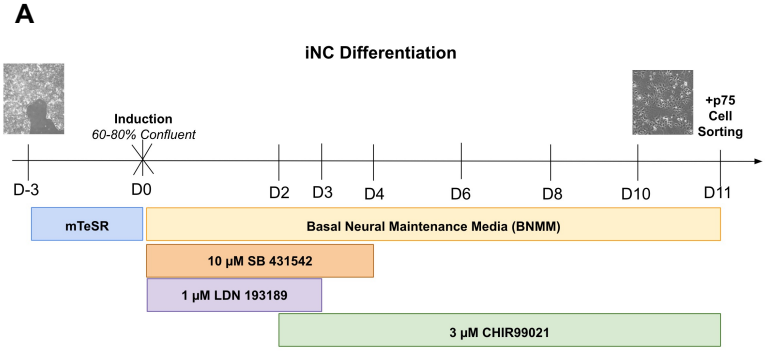
A
iNC Differentiation
Induction
60-80% Confluent
+p75
Cell
Sorting
D-3
D0
D2
D3
D4
D6
D8
D10
D11
mTeSR
Basal Neural Maintenance Media (BNMM)
10 µM SB 431542
1 µM LDN 193189
3 µM CHIR99021

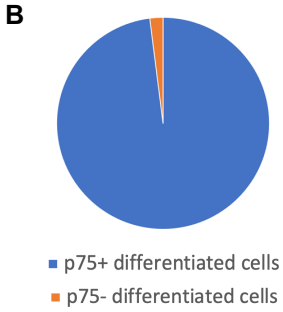
B
p75+ differentiated cells
p75- differentiated cells

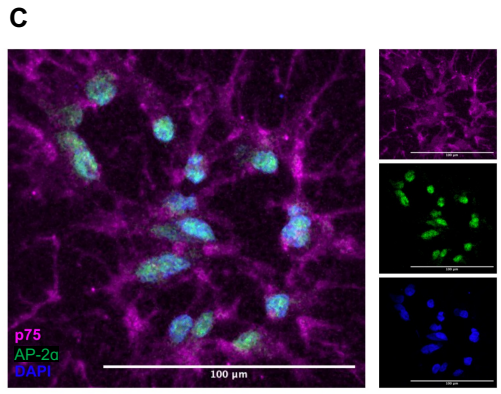
C
p75
AP-2α
DAPI
100 µm

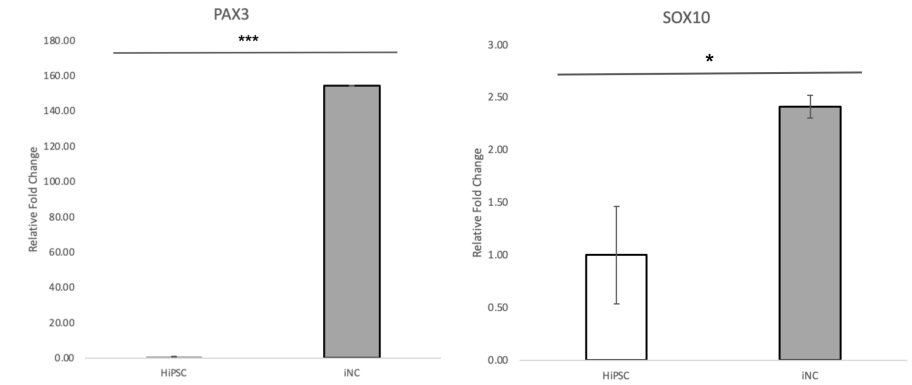
D
PAX3
***
Relative Fold Change
HiPSC
iNC
SOX10
*
Relative Fold Change
HiPSC
iNC

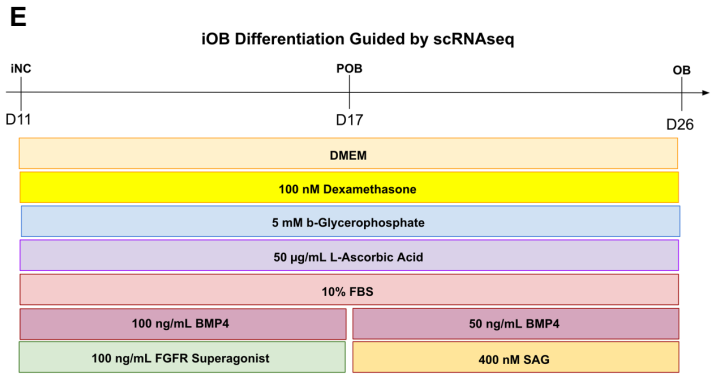
E
iOB Differentiation Guided by scRNAseq
iNC
POB
OB
D11
D17
D26
DMEM
100 nM Dexamethasone
5 mM b-Glycerophosphate
50 µg/mL L-Ascorbic Acid
10% FBS
100 ng/mL BMP4
50 ng/mL BMP4
100 ng/mL FGFR Superagonist
400 nM SAG

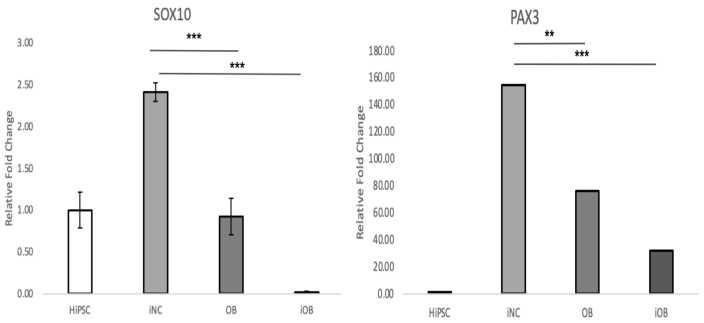
F
SOX10
***
***
Relative Fold Change
HiPSC
iNC
OB
iOB
PAX3
**
***
Relative Fold Change
HiPSC
iNC
OB
iOB

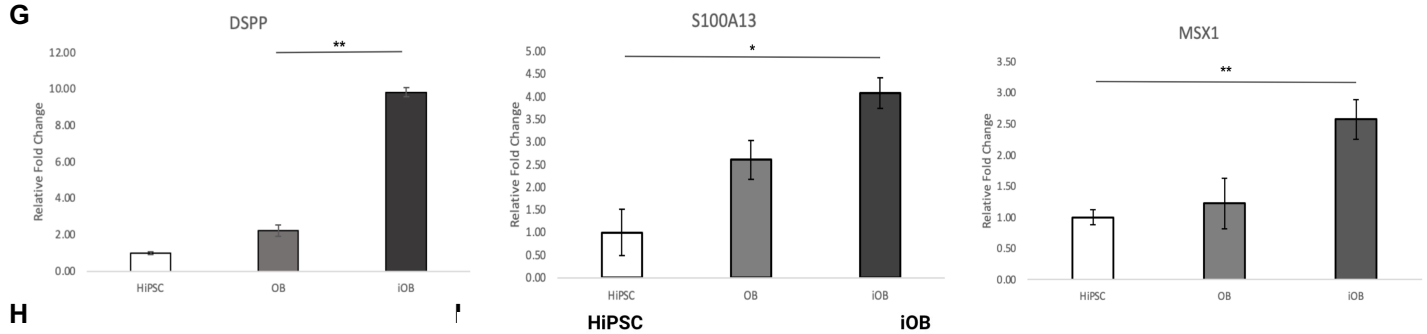
G
DSPP
**
Relative Fold Change
HiPSC
OB
iOB
S100A13
*
Relative Fold Change
HiPSC
OB
iOB
MSX1
**
Relative Fold Change
HiPSC
OB
iOB

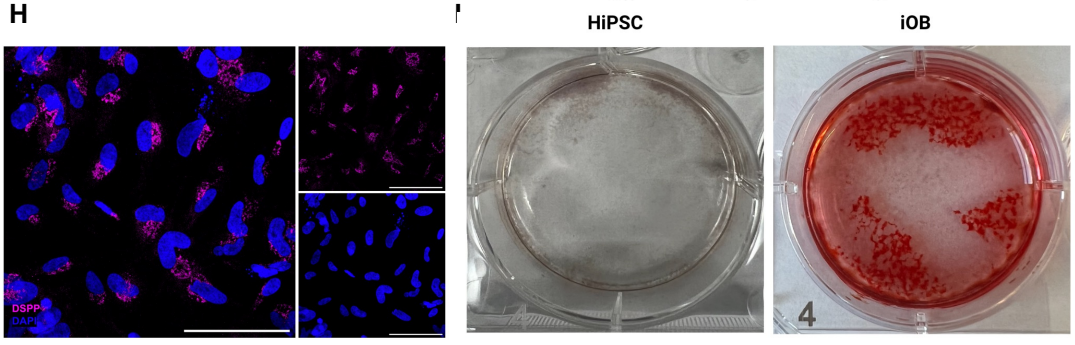
H
I
HiPSC
iOB
DSPP
DAPI
4

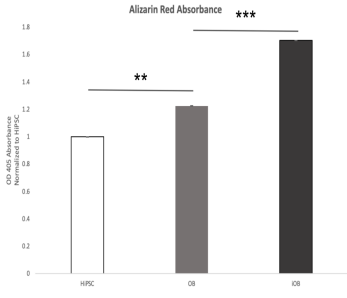
Alizarin Red Absorbance
***
**
HiPSC
OB
iOB

Figure 5. HiPSC-derived odontoblast differentiation guided by sci-RNA-seq (iOB) produces mature odontoblast cells. (A) Schematic of the 11-day neural crest differentiation protocol (iNC) as described previously (Studer). (B) 98% of cell differentiated towards neural crest fate express neural crest marker p75 (CD271) as assessed by magnetic cell sorting. (C) Immunofluorescence staining of iNC show expression of neural crest markers p75 in the cytoplasm and AP-2α localized to the nucleus. (D) iNC show upregulated expression of neural crest markers PAX3 and SOX10 as assessed by QRT-PCR compared to undifferentiated HiPSC control. Each study was performed in triplicate, with error bars representing SEM. (E) Schematic of the 15-day differentiation protocol produced, which targets the identified signalling pathways utilizing growth factors and small molecules to transition through the odontoblast developmental trajectory. iNC cultured in odontogenic media and treated with FGFR superagonist minibinder (iOB) show decreased expression of neural crest markers PAX3 and SOX10 (F) and upregulated expression of odontoblast markers MSX1, DSPP and S100A13 (G) as assessed by QRT-PCR compared to undifferentiated HiPSC control. Each study was performed in triplicate, with error bars representing SEM. (H) Immunofluorescence staining of iOB shows DSPP present in the cytoplasm or secreted from the cell. (I) HiPSC and iOB were stained for
extracellular calcifications with Alizarin Red Stain. Spectrometric quantification of Alizarin stain normalized to HiPSC control shows iOB have enhanced mineralization capacity. *$p < 0.05$;**$p < 0.01$; ***$p<0.001$.

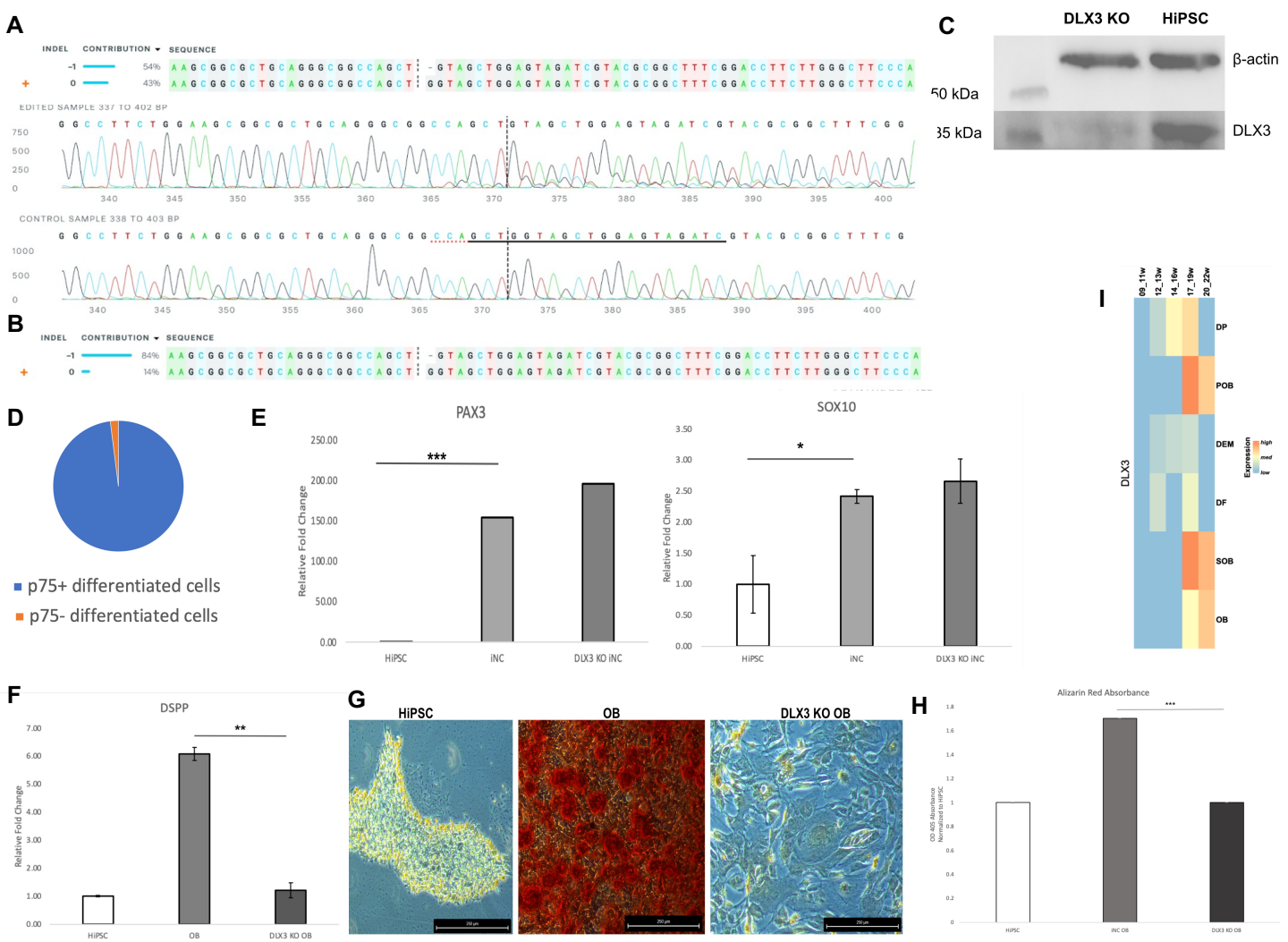

Figure 6. Loss of disease associated transcription factor DLX3 inhibits odontoblast maturity in vitro. Sanger sequencing results of DLX3 knock-out mutant line compared to HiPSC shows initial 54% of cells possess a single base pair deletion at site 374 with removal of a single glycine nucleotide. This population transitions to 84% after odontoblast differentiation (B). Solid black line indicates guide RNA (gRNA) sequence; black dotted line indicates cut site; red dotted line indicates PAM sequence. (C) Presence of DLX3 protein was evaluated by Western Blot, showing loss of protein in the mutant line. (D) Mutant cells were differentiated towards neural crest fate as described previously and showed the same 98% efficiency of producing p75+ cells during magnetic cell sorting. DLX3 mutants show unchanged expression of neural crest markers PAX3 and SOX10 compared to iNC (E) with significantly decreased expression of odontoblast marker DSPP (F) compared to iOB as assessed by QRT-PCR. Each study was performed in triplicate, with error bars representing SEM. The loss of DLX3 on mineralization capacity was evaluated by Alizarin Red Staining (G). Spectrometric quantification of Alizarin stain normalized to HiPSC control shows DLX3 mutants have mineralization capacity similar to control (H). (I) DLX3 expression in human dental ectomesenchyme derived cells over time. *p < 0.01; ***p<0.001*.

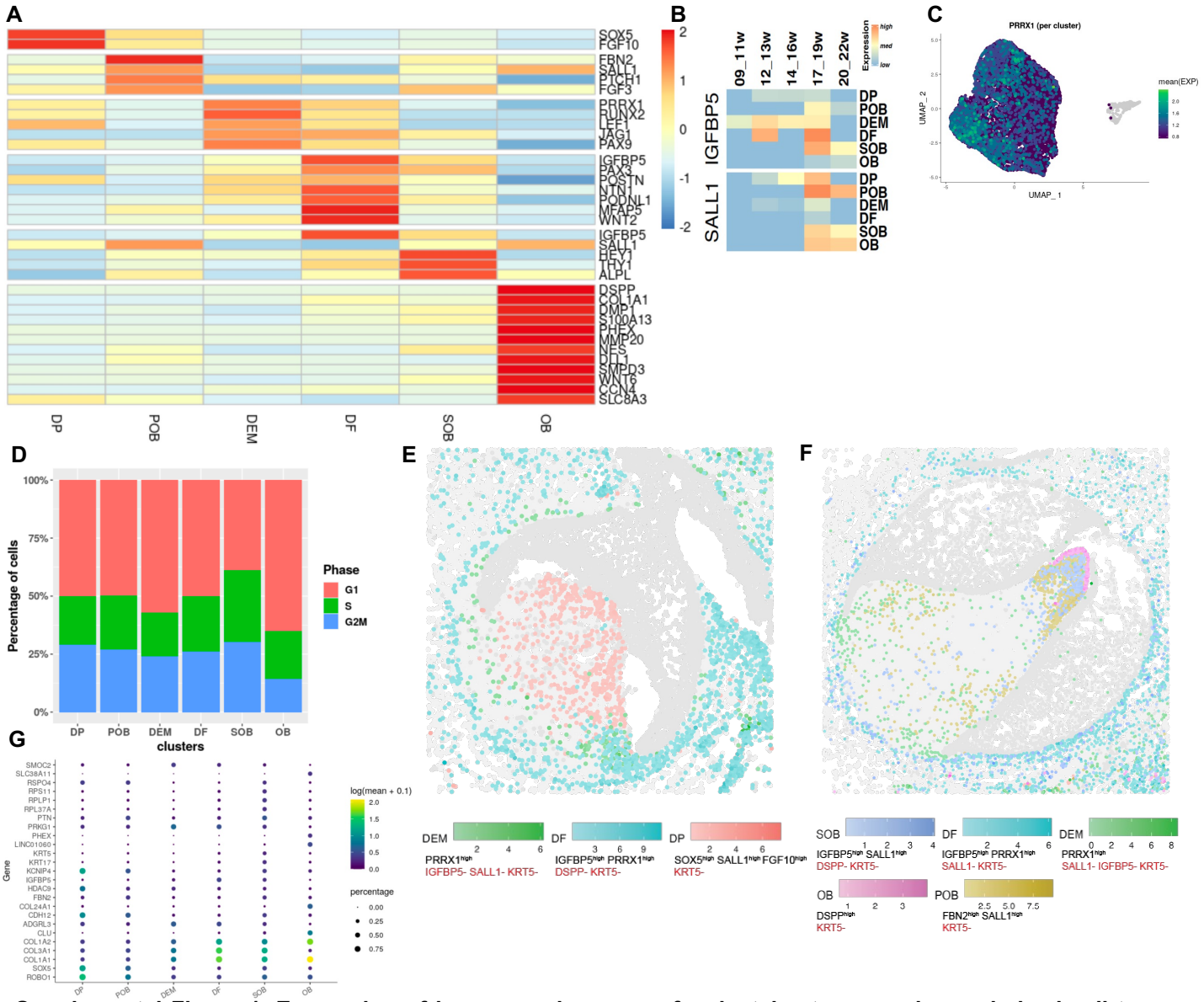

Supplemental Figure 1. Expression of known marker genes for dental ectomesenchyme derived cell types. (A). Heatmap of known marker gens for dental ectomesenchyme derived cell types. (B). Heatmap of expression over time of dental follicle marker IGFBP5 and subodontoblast markers SALL1 (C). Gene density plot of shared DP and DEM progenitor marker PRRX1 (D). Cell cycle scoring of dental mesenchyme derived cell types. Mappings for dental mesenchyme-derived cell types at 80d replicate (E) and 117d replicate (F) identified by analysis of RNAscope images which show mapping for SOB, DF, DEM, OB, and POB cell types. (G) Top marker genes for dental ectomesenchyme derived cell types .

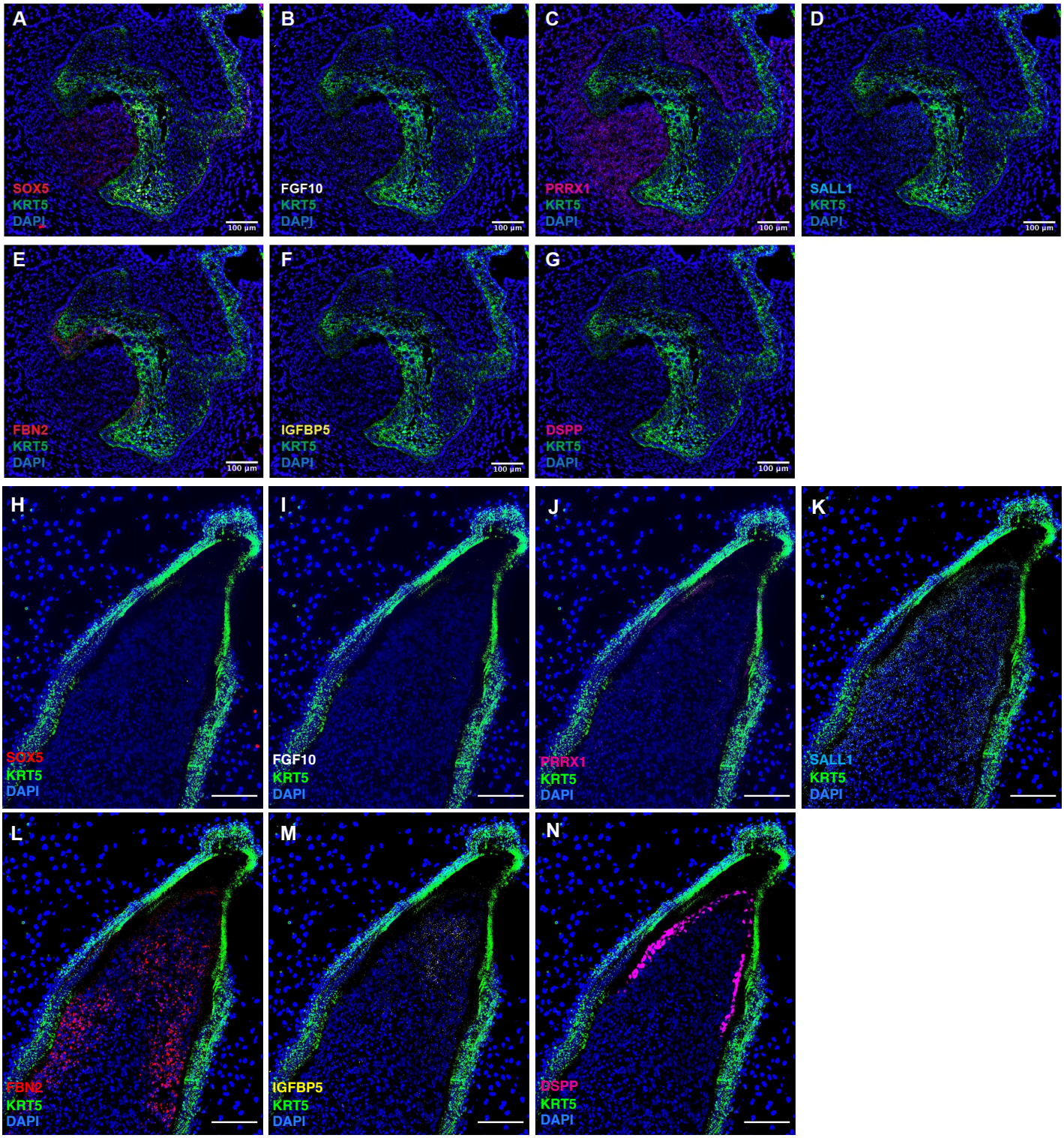

Supplemental Figure 2. Individual channels of merged RNAScope images in Fig 2F and H. A and H) SOX5; B and I) FGF10; C and J) PRRX1; D and K) SALL1; E and L) FBN2; F and M) IGFBP5; G and N) DSPP in 80d and 117d incisor toothgerms respectively. Scale bar = 100 µm.

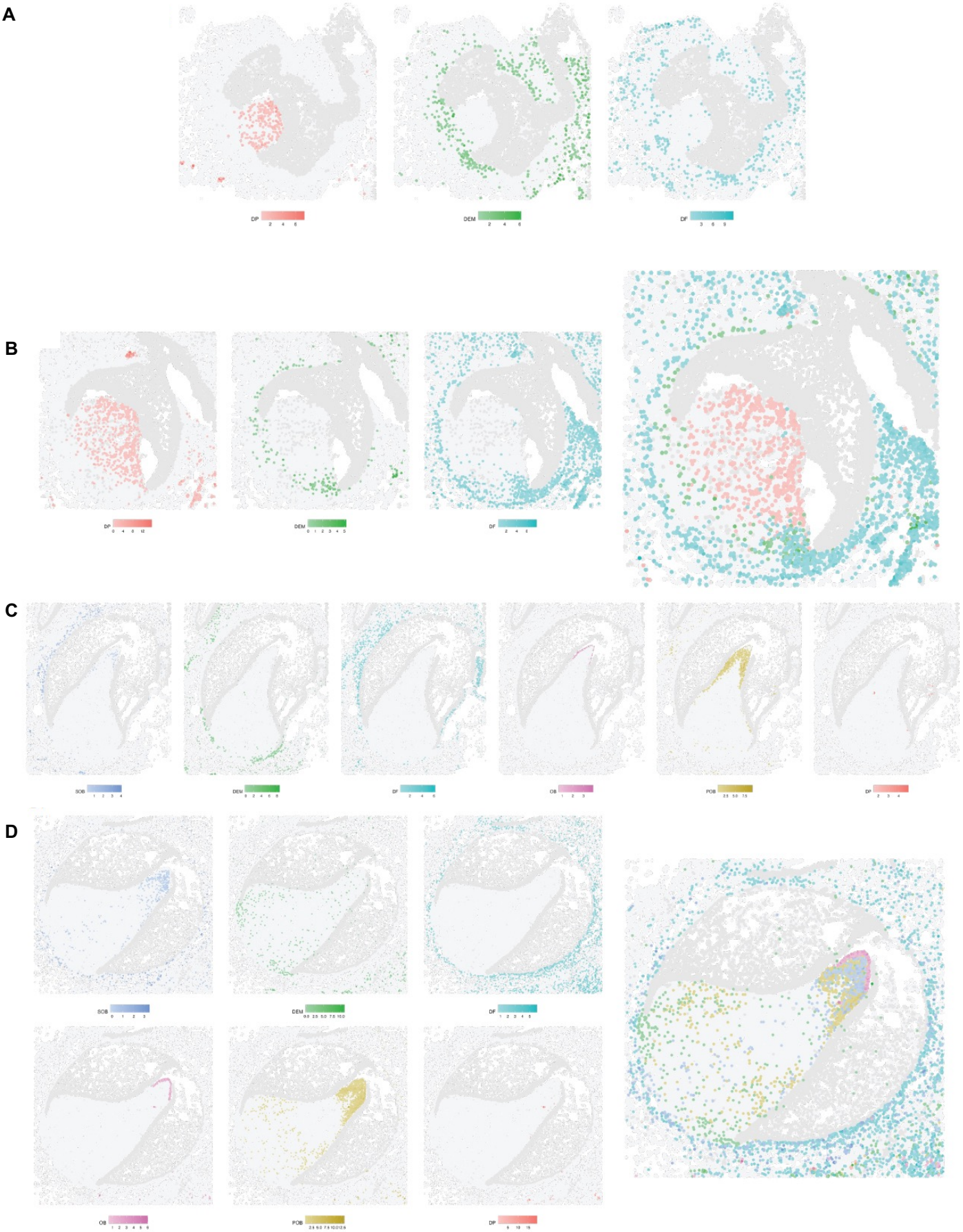

Supplemental Figure 3. Individual channels of mapped RNAScope replicate images in Fig 2F and H. Mappings for dental mesenchyme-derived cell types at 80d replicate (A and B) and 117d replicate (C and D) identified by analysis of RNAscope images which show mapping for SOB, DF, DEM, OB, and POB cell types.

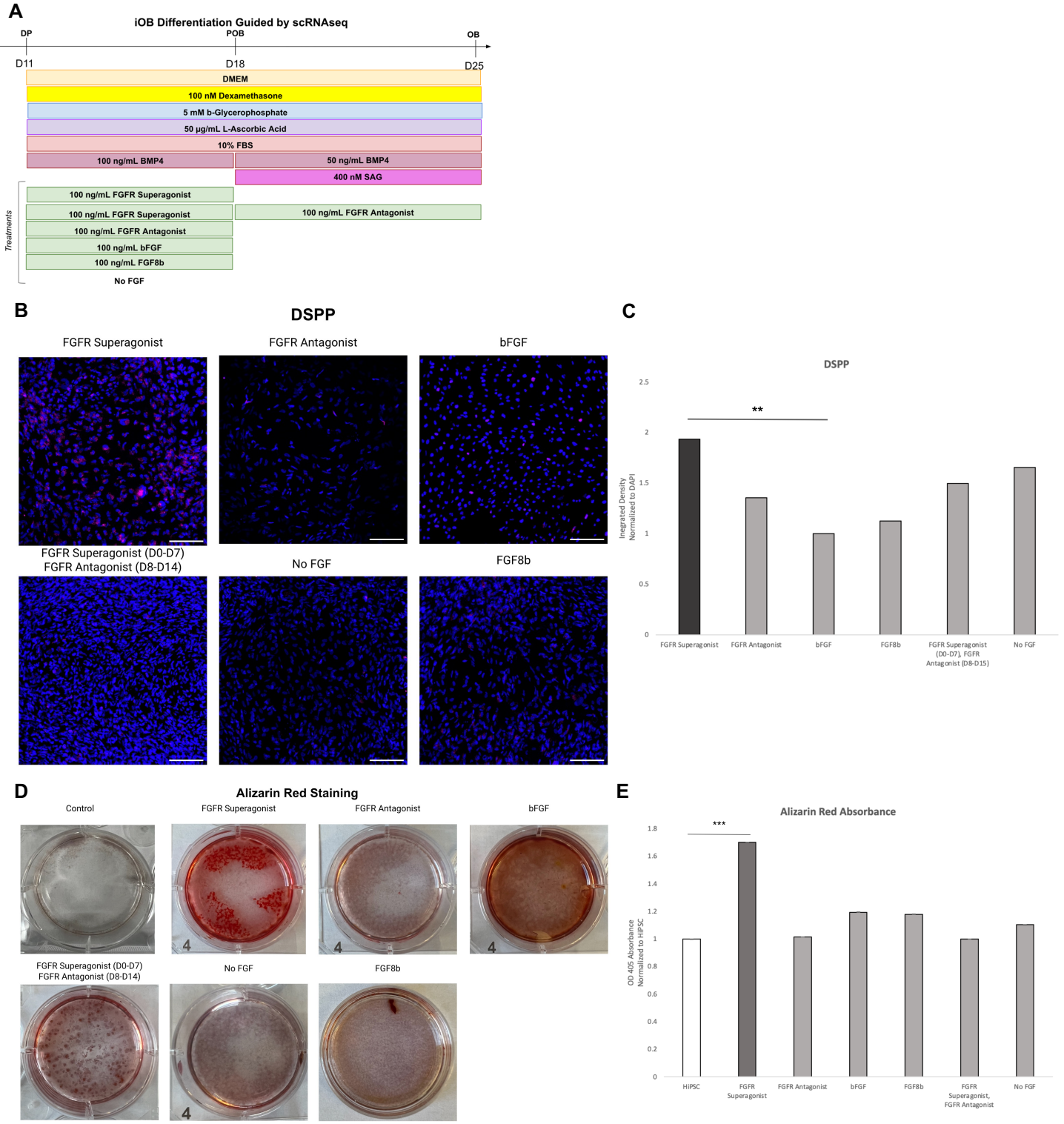

Supplemental Figure 4. Expression of DSPP protein and mineralization capacity of various odontoblast treatments. (A) Schematic of the 15-day differentiation protocol produced, which targets the identified signaling pathways utilizing growth factors and small molecules to transition through the odontoblast developmental trajectory. Treatments activated FGF signaling by supplementation of media with either FGFR superagonist minibinder, basic FGF (bFGF or FGF2), FGF8b; inhibited FGF signaling by supplementation of media with FGFR antagonist minibinder; or were not treated with FGF. (B) Immunofluorescence staining of treated cells shows DSPP present in cells treated with FGFR superagonist. (C) Quantification of DSPP integrated density normalized to DAPI shows a two-fold increase in DSPP expression in cells treated with FGFR superagonist compared to those treated with bFGF. (D) Differentiated cells were stained for extracellular calcifications with Alizarin Red Stain. (E) Spectrometric quantification of Alizarin stain normalized to HiPSC control shows iOB treated with FGFR superagonist have significantly increased mineralization capacity. *p < 0.01; ***p<0.001*.

CURRICULUM VITAE

NAME: **Sesha Hanson-Drury**

eRA COMMONS USER NAME (credential, e.g., agency login): **seshahd**

POSITION TITLE: **DDS/PhD Graduate Trainee**

EDUCATION/TRAINING

INSTITUTION AND LOCATION	**DEGREE** *(if applicable)*	**Start Date MM/YYYY**	**Completion Date MM/YYYY**	**FIELD OF STUDY**
SUNY Stony Brook University	NA	08/2007	05/2008	Biology
Columbia Basin Community College	AA with High Honors	06/2008	06/2008	Biology
Western Washington University	BS	04/2009	12/2011	Biological Anthropology
University of Washington School of Dentistry (UWSOD)	DDS	08/2015	06/2019	Dentistry
University of Washington	PhD	06/2019	Current	Oral Health Sciences

A. Personal Statement

My passion for research was ignited as a high school junior in the Robert Wood Johnson Foundation's Young Epidemiology Scholars competition. Science provided me with the tools to answer something previously not known, and being a finalist in the competition allowed me to experience the knowledge sharing and camaraderie of a scientific conference for the first time. I was hooked. My gusto for conducting science and disseminating knowledge has only grown through my experience as a Research Associate at the Pacific Northwest National Laboratory and as a student in the dual DDS/PhD at the University of Washington School of Dentistry.

The impact of translational research on my patient population became clear to me upon my simultaneous research rotation performing genetic sequencing of the periodontal pathogen *Tannerella forsythia* under Dr. Jeffrey McLean and treating patients in the dental clinic at various stages of the "tooth cycle of death", wherein a tooth with a cavity is restored with a filling, which then has a recurrent cavity requiring further restoration, until a tooth finally requires removal and replacement with a dental implant. This coupled experience in genetic sequencing and desire to provide patients with clinical restorations that would exit them from the "tooth cycle of death" bloomed my interest in the field of regenerative dentistry.

I began studying development and cell fate commitment via human induced pluripotent stem cell differentiation under Dr. Hannele Ruohola-Baker at the Institute for Stem Cell and Regenerative Medicine (ISCRM). In addition to state-of-the-art facilities and training, as a member of the Ruohola-Baker lab I am also a member of the ISCRM community, which is rich with opportunities to develop into a productive and

independent dentist-scientist through oral research presentation, biomedical ethics, and interdisciplinary collaboration. I have also had the opportunity to mentor multiple undergraduate and dental students through research rotations in our lab, which has cemented my desire to continue teaching academically and foster a diverse community of incoming dentists and researchers.

My long-term research interests involve the development and cell fate commitment of odontogenic cells in order to regenerate oral tissues, and how disruption of these processes contribute to human oral disease. Ultimately, my goal as a dentist-researcher is to remain in academia. I intend to pursue a tenure-faculty track where I am able to have my own lab, teach, and practice evidence-based dentistry. The training described in this proposal will aid me in becoming an academic clinician who will have a profound impact on patient's lives through cutting edge treatment; the next generation of students through passionate education; and the field of regenerative dentistry by supporting an active member of the community.

Citations:

1. **Hanson-Drury S**, et al. The signaling pathways that determine human tooth germ type: FGF is critical to odontoblast formation and incisor vs molar formation. Manuscript in preparation.
2. Alghadeer A, **Hanson-Drury S**, et al. Human iPSC Derived Enamel Organoid Guided by Single Cell Atlas of Human Tooth Development. Cell Stem Cell, Manuscript submitted July 2022.
3. Ehnes, D, Alghadeer A, **Hanson-Drury S**, et al. Sci-Seq of human fetal salivary tissue introduces human transcriptional paradigms and a novel cell population. Frontiers in Dental Medicine. Manuscript submitted March 2022.
4. **Hanson-Drury S**, To TT, Liu Q, Vo AT, Kim M, Watling M, Bumgarner RS, Mclean JS. Draft genome sequence of *Tannerella forsythia* clinical isolate 9610. Genome announcements. 2017 Mar 23;5(12).

B. Positions and Employment

ACTIVITY/ OCCUPATION	INSTITUTION	FIELD	START DATE MM/YYYY	END DATE MM/YYYY	SUPERVISOR / EMPLOYER
Dental Associate	Bainbridge Dental	General Dentistry	02/2020	Current	Nicholas Thompson, DMD
Doctoral Trainee	ISCRM	Regenerative Dentistry	06/2018	Current	Hannele Ruohola-Baker, PhD
Research Fellow	UWSOD	Periodontics	06/2016	03/2017	Jeffrey Scott McLean, PhD
Dental Assistant	Seattle Dental	General Dentistry	10/2013	05/2015	Joseph Zimmer, DDS, MAGD

Research Associate	PNNL	Toxicology	11/2011	03/2013	Justin Teeguarden, PhD

Academic or Professional Honors

AWARD, HONOR OR SCHOLARSHIP	SPONSORING ORGANIZATION	YEAR RECEIVED
Fellow	Achievement Rewards for College Scientists (ARCS) Foundation	2019
Outstanding Senior Award	American Academy of Orofacial Pain	2019
Quintessence Award for Clinical Achievement in Research	UWSOD	2019
Service Award	UW Office of Educational Partnerships & Diversity	2019
Graduate Student Poster Competition, 3rd Place	UWSOD	2017
Psi Omega Scholar	UWSOD	2016, 2017
Top Scholar Award	UW Graduate School Fund for Excellence and Innovation	2015
Perry J. Gehring Award	Society of Toxicology	2013
Undergraduate Poster Competition, 1st Place	PNNL	2011
President's List	Western Washington University	2010
Honors Program	Western Washington University	2009-2011
President's List	Columbia Basin College	2008
Dean's List	SUNY Stony Brook University	2007
Women In Science and Engineering Fellowship	SUNY Stony Brook University	2007-2008
Young Epidemiology Scholars, Regional Finalist	Robert Wood Johnson Foundation	2006

Professional Memberships

International Association for Dental Research
American Dental Association
Seattle-King County Dental Association
International Society for Stem Cell Research
Washington State Dental Association
Washington Academy of General Dentistry

C. Contributions to Science

1. **High School Research:** Under the mentorship of Dr. Joseph Montgomery at Columbia Basin College I designed a complex survey instrument that was reliable, tested my hypothesis, and factored important metrics (e.g. social interactions, body mass index, health status); implemented the survey to approximately 80 high school students; performed statistical analysis; and presented the results of my first study.

a. **Hanson-Drury S**, Montgomery J. Dating and Friendship Relationships and Overweight/Obesity Status: Significant Associations in High School Students. Young Epidemiology Scholars Competition; Washington, DC; 2006.

2. **Undergraduate Research:** As an undergraduate accepted into the PNNL's Student Undergraduate Laboratory Intern program in Dr. Richard Corley's lab, I planned and implemented multiple molecular and biological techniques to develop the pharmacokinetic parameters to describe metabolism of carcinogens benzo[a]pyrene (B[a]P) and dibenzo[def,p]chrysene (DBC) in rodents and humans. I independently performed rodent dissections, synthesized microsomes, and completed general metabolism studies involving extractions and high-performance liquid chromatography analysis. During my time in the lab, I obtained kinetic parameters that were critical to revising preliminary physiologically based pharmacokinetic (PBPK) models to facilitate extrapolations to realistic human exposures.
    a. **Hanson-Drury S**, Crowell SR, Soelberg J, Williams DE, Corley R. *In Vitro* Metabolism of Benzo[a]pyrene and Dibenzo[def,p]chrysene in Rodents and Humans. Pacific Northwest National Laboratory Undergraduate Poster Competition; Richland, WA; 2011.

   Upon completion of my undergraduate degree, I returned to PNNL as a Research Associate. In addition to my continued work in Dr. Corley's lab on the *in vitro* metabolism of B[a]P and DBC and development of mammalian life stage PBPK models, I joined Dr. Justin Teeguarden's lab executing a systematic review of "low dose" Bisphenol A health effect studies, collecting, organizing, and presenting exposure/dosimetry data to establish a standard for reporting toxicity data based on human exposure, rather than subjective terms such as "low dose".
    b. Teeguarden JG, **Hanson-Drury S**. A systematic review of Bisphenol A "low dose" studies in the context of human exposure: A case for establishing standards for reporting "low-dose" effects of chemicals. Food and chemical toxicology. 2013 Dec 1;62:935-48.
    c. Teeguarden JG, **Hanson-Drury S**, Fisher JW, Doerge DR. Are typical human serum BPA concentrations measurable and sufficient to be estrogenic in the general population? Food and chemical toxicology. 2013 Dec 1;62:949-63.
    d. Crowell SR, **Hanson-Drury S**, Williams DE, Corley RA. *In vitro* metabolism of benzo [a] pyrene and dibenzo [def,p] chrysene in rodent and human hepatic microsomes. Toxicology letters. 2014 Jul 3;228(1):48-55.

3. **Graduate Research:** As a dual PhD/DDS student at the UWSOD I rotated in Dr. Jeffrey McLean's lab to study *Tannerella forsythia*, one of three members of the "red-complex" of periopathogens associated with development of periodontitis. Due to *T. forsythia's* fastidious growth requirements, relatively little was known of its inter-microbial relationships and virulence mechanisms. I cultured, sequenced and performed comparative genomics of *T. forsythia* clinical isolate 9610. This work identified and phylogenetically placed a novel draft genome sequence of *T. forsythia* clinical isolate 9610. Importantly, I identified the presence of

valine-glycine repeat protein G, a puncturing component of the type VI secretion system used by Gram-negative bacteria to deliver effectors unto target cells via direct cell-cell contact. This study significantly provides insights that enables further study into the role of *T. forsythia* in the initiation and progression of periodontal disease.

a. **Hanson-Drury S**, To TT, Liu Q, Vo AT, Kim M, Watling M, Bumgarner RS, Mclean JS. Draft genome sequence of *Tannerella forsythia* clinical isolate 9610. UWSOD Graduate Poster Competition; Seattle, WA; 2017 and International Association of Dental Research; San Francisco, CA; 2017.

In my 4th year of dental school, I rotated in Dr. Hannele Ruohola-Baker's lab at the UW Institute for Stem Cell and Regenerative Medicine studying the signaling pathways involved in the induction and differentiation of ameloblasts, the oral epithelium derived cells responsible for enamel secretion. Loss of dental enamel is irreversible in nature due to the death of ameloblasts following tooth eruption. I developed a novel differentiation protocol for human induced pluripotent stem cells (HiPSC) to oral epithelium. This project importantly produced a consistent and efficient maintenance, culture, and differentiation protocol; determined key molecular signaling factors bone morphogenic protein 4 (BMP4), smoothened agonist (SAG), and fibroblast growth factor 10 (FGF10) in the differentiation process; and identified unique transcription factor *Pitx2* expressed by mature oral epithelial cells. Identifying key differentiation signaling molecules involved and specific markers for the oral epithelium significantly took the dental regenerative field one step closer to bioengineering enamel from HiPSC derived ameloblasts.

b. **Hanson-Drury S**, Alghadeer A, Zhao YT, Mathieu J, Ruohola-Baker H. From HiPSC to Oral Epithelium: Identifying the Signaling Molecules Required to Generate Oral Epithelium from Human Induced Pluripotent Stem Cells. UW Graduate Research Day; Seattle, WA; 2019.

Upon completion of my DDS, I joined Dr. Ruohola-Baker's lab as a PhD doctoral candidate where I continued my study of the signaling patterns responsible for tooth development with the long-term goal of bioengineering natural tooth structure. My current work generates a novel single cell atlas to assess transcriptome heterogeneity and delineate cell lineage relationships in early development, differentiation, and fate determination in the tooth germ via single-cell combinatorial indexing RNA sequencing (sci-RNA-seq). The differential gene expression observed in the ameloblast and odontoblast (the ectomesenchyme derived cells responsible for dentin secretion) highlights the transcriptional regulation of their differentiation and the need to identify the underlying regulatory mechanisms involved in order to characterize these highly specialized cell types, develop therapeutic practices, and optimize a novel differentiation protocol of HiPSC to odontoblasts to produce a tooth organoid.

a. Alghadeer A, **Hanson-Drury S**, et al. A preliminary human gene expression atlas of human tooth and salivary gland development via sci-RNA-seq. Tooth Morphogenesis and Differentiation Conference; Oxford, UK; 2019.

b. **Hanson-Drury S**, et al. The developing odontoblast: a novel single cell gene expression atlas of human fetal tooth germ via sci-RNA-seq. International Society for Stem Cell Research (ISSCR). Virtual, 2020.
c. **Hanson-Drury S**, et al. The developing human odontoblast: unraveling progenitor sources and spatiotemporal signaling via single cell RNA sequencing. ISSCR. Virtual, 2021.
d. **Hanson-Drury S**, et al. The developing human odontoblast: unraveling progenitor sources and spatiotemporal signaling via single cell RNA sequencing. UW OHS Seminar. Virtual, 2021.

D. Additional Information: Scholastic Performance

UNIVERSITY OF WASHINGTON SCHOOL OF DENTISTRY				
YEAR	**COURSE TITLE**	**GRADE**	**COURSE TITLE**	**GRADE**
2015	EARLY CLIN IMMERSN	CR	ORAL MICROBIO	3.8
	MOL CEL DISEASE	CR	DENTAL ANATOMY	3.4
	INVDERS & DFNDERS	CR	INTRO TO PERIO	4.0
	FNDN OF DENTAL MED	4.0	HEALTH IN HOMELESSNESS	CR
2016	CARD PULM RENL DIS	CR	OPERATIVE DENT 2	3.6
	INTRO DENT PUB HLTH	4.0	IMMEDIATE DENTURES	3.5
	FNDNS DNTAL MED 2	4.0	LOCAL ANESTHESIA	3.9
	ORAL HIST & EMB 1	3.6	ORAL PATHOLOGY 1	3.6
	DENTAL OCCLUSION	3.7	RMV PART DENT DESIGN	3.7
	HEALTH IN HOMELESSNESS	CR	H-P-DIR STUDYS PERIO	CR
	P-DIR STUDYS IN RESD	CR	MIND BRAIN BEHAVIOR	CR
	RESEARCH SEMINAR	CR	LIFECYCLE & REPRO	CR
	BLOOD & CANCER	CR	FNDNS DENTAL MED 3	3.8
	ENERGY & HOMEOSTASIS	CR	OPERATIVE DENT 3	3.4
	ORAL HIST & EMB 2	4.0	FIXED PROS I	3.7
	INTRO OPER DENT	3.6	CMPLT DENTURES 1	3.8
	EVIDENCE-BASED DENT	3.7	DENT PRAC CONVRSTNS	CR
	RADIOLOGY THEORY	3.3	NAT BOARD REVIEW	CR
	HEALTH IN HOMELESSNESS	CR	HEALTH IN HOMELESSNESS	CR
2017	DENT PRAC CONVRSTNS	CR	ORTHODONTICS 2	4.0
	OPERATIVE DENT 4	3.9	INTRO ENDODONTICS	3.8
	FIXED PROS 2	3.5	RMV PART DENTURES 2	3.9
	COMPLT DENTURES 2	3.5	INT PEDIATRIC DENT	3.8
	ORTHODONTICS 1	3.3	PERIODONTICS 3	4.0
	ORAL PATHOLOGY 2	3.3	PT ADVOCACY	4.0
YEAR	**COURSE TITLE**	**GRADE**	**COURSE TITLE**	**GRADE**
2017 cont.	RMV PART DENTURES I	3.7	HEALTH IN HOMELESSNESS	CR
	CLIN ORAL RADIOLOGY	3.9	PROS CLERKSHIP	3.7
	PERIODONTICS 2	3.8	PERIO CLERKSHIP	3.7

	HEALTH IN HOMELESSNESS	CR	PT ADVOCACY	4.0
	P-DIR STDYS IN RESD	CR	HEALTH IN HOMELESSNESS	CR
	DENT PRAC CONVRSTNS	CR	FOUNDATIONS OF IPE	CR
	OPERATIVE DENT 5	3.5	OMS CLERKSHIP	4.0
	FIXED PROS 3	3.6	PEDO ORTH CLERKSHIP	3.8
	IMPLANT DENTISTRY	3.9	PT ADVOCACY	4.0
	HEALTH IN HOMELESSNESS	CR		
2018	FOUNDATIONS OF IPE	CR	HEALTH IN HOMELESSNESS	CR
	DXTX CLERKSHIP	3.9	ADV TOP GEN DENT 2	4.0
	ORALM CLERKSHIP	4.0	GEN DENT CLINIC 2	4.0
	PT ADVOCACY	4.0	TX PT SPC ND CLIN 2	CR
	HEALTH IN HOMELESSNESS	CR	DENT URGENT CARE 2	4.0
	FOUNDATIONS OF IPE	CR	DENTAL PHOTOGRAPHY	CR
	ENDO CLERKSHIP	3.7	P-DIR STDYS IN O D	CR
	OPER CLERKSHIP	3.8	HEALTH IN HOMELESSNESS	CR
	PT ADVOCACY	4.0	ADV CONE BEAM CT	CR
	ADV TOPICS GEN DENT	3.5	INTRO TO CAD/CAM	CR
	P-DIR STUDYS DPHS	CR		
2019	SERV LEARN ROTATION	3.8	4TH YEAR CLIN COMPS	CR
	ADV TOP GEN DENT 3	4.0	SURGICAL PERIO	CR
	GEN DENT CLINIC 3	3.9	CLINIC MAGNIFICATION	CR
	TX PT SPC ND CLIN 3	CR	DIRECT GOLD RESD	CR
	DENT URGENT CARE 3	4.0	BIOSTAT IN DENTISTRY	3.8
	ADV TOP GEN DENT 4	4.0	RESEARCH TECHNIQUES	4.0
	GEN DENT CLINIC 4	3.8	MOLECULAR BIOLOGY	3.7
	TX PT SC ND CLIN 4	CR	OHS SEMINAR	CR
	DENT URGENT CARE 4	4.0	RESEARCH TECHNIQUES	4.0
	ORAL IMMUNOLOGY	3.7		
2020	ADV ORAL MICRO	4.0	DIRECTING STEM CELLS	4.0
	OHS SEMINAR	CR	INDEPENDENT STDY/RSCH	4.0
2021	MOLECULAR BIOLOGY LAB	4.0	OHS SEMINAR	CR
	DOCTORAL DISSERTATION	4.0		
2022	DOCTORAL DISSERTATION	4.0	OHS SEMINAR	CR

UWSOD grades using a 4.0 scale with letter equivalents. A=3.0-3.9, A-=3.8-3.5, B+=3.4-3.2, B=3.1-2.9, C+=2.4-2.2, C=2.1-1.9, C-=1.8-1.5, D+=1.4-1.2, D=1.1-0.9, D-=0.8-0.7, E=0.0. Some courses were credit/no credit (CR/NC). Passing is C or better. Grades for courses lasting longer than one quarter (QTR) were averaged.